



Proteolysis targeting chimera of BI-2536 induces potent dual degradation of PLK1 and BET proteins

Shiwei Song, Wanrong Yang, Wanyi Tai^{*} 

Department of Pharmaceutical Engineering, School of Pharmaceutical Sciences, Wuhan University, Wuhan, Hubei 430071, China

ARTICLE INFO

Keywords:

Dual-targeting PROTAC
BRD4
BI-2536
PLK1
BET protein

ABSTRACT

Polo-like kinase 1 (PLK1) and bromodomain 4 (BRD4) are well-known oncoproteins that drive tumor cell growth in many cancer types. Simultaneously targeting these protein targets has been intently pursued by scientists to enhance anti-cancer effect in chemotherapy. However, it is rare to design proteolytic targeting chimeras (PROTAC) to degrade these oncoproteins simultaneously by one single molecule. Herein, we designed and synthesized seven PROTAC molecules based on BI-2536, a dual-target inhibitor of BRD4 and PLK1. Among these, compound 17b demonstrated the best ability to degrade PLK1, BRD4 and other BET family proteins. The dual targeting PROTAC 17b induces the almost complete degradation of BET proteins and PLK1 at concentration as low as 3 nM, but proteolysis of PLK1 takes place a lot later than BET proteins (36 h vs 4 h). Compound 17b exhibited strong anti-proliferative activities across multiple cancer cell lines. Furthermore, 17b was able to regulate the expression of downstream genes involved in key cellular processes and exert the prolonged suppression of cancer cell growth. These findings suggest that 17b is a highly potent and efficacious dual-targeting degrader.

1. Introduction

In recent decades, scientists have persistently sought innovative drug therapies aimed at enhancing the efficacy of disease treatments and improving the quality of life for patients.¹ In this quest, a groundbreaking drug development strategy known as Proteolysis Targeting Chimeras (PROTAC) has gained substantial attention.² Initially proposed by Yale University professor Craig Crews and his colleagues in 2001, PROTAC technology leverages the body's intrinsic protein degradation mechanism to decrease protein levels, rather than simply inhibiting protein function.³ Over two decades of development, PROTAC has evolved into a leading-edge technology in drug research and development. It has garnered widespread favor among research institutions, pharmaceutical companies, and investors due to its novel approach and potential to address previously undruggable targets. This widespread adoption underscores the transformative impact of PROTAC on the therapeutic development.⁴

PROTAC technology functions through the interaction of two distinct ligands: one ligand specifically binds to the target protein, referred to as the protein of interest (POI), while the other ligand attaches to a ubiquitin ligase, most often designated as E3.⁵ Upon simultaneous binding of

both the POI and E3 by PROTAC molecule (ternary complex), a process of ubiquitination is initiated.⁶ This process involves tagging the target protein with ubiquitin, a small regulatory protein. Consequently, the tagged protein is recognized and degraded by the ubiquitin–proteasome system (UPS), a cellular mechanism responsible for protein catabolism (Fig. 1). Notably, the PROTAC molecule is not consumed in this process but can be recycled for repeated use.⁷ This mechanism contrasts sharply with the traditional 'one-to-one' interaction paradigm of small molecule drugs and their target proteins.⁸ Instead, PROTAC operates on a 'one-to-many' basis, facilitating the degradation of multiple protein molecules with a single PROTAC molecule, thereby enhancing the efficiency of protein degradation.⁹

Over the past decade, the PROTAC strategy has achieved significant advancements in the targeted degradation of proteins, particularly within the Bromodomain and Extra-Terminal domain (BET) family.¹⁰ The BET family, encompassing members such as BRD2, BRD3, BRD4, and BRDT, plays a pivotal role in epigenetic regulation.¹¹ These proteins bind to acetylated histones via their bromodomains, thereby localizing to chromatin and regulating both the initiation and elongation phases of gene transcription.¹² Among the BET proteins, BRD4 has garnered the most attention due to its substantial role in the regulation of critical

^{*} Corresponding author.

E-mail address: wanyi-tai@whu.edu.cn (W. Tai).

<https://doi.org/10.1016/j.bmc.2025.118087>

Received 29 October 2024; Received in revised form 5 January 2025; Accepted 23 January 2025

Available online 28 January 2025

0968-0896/© 2025 Elsevier Ltd. All rights are reserved, including those for text and data mining, AI training, and similar technologies.

genes involved in cell proliferation, differentiation, and survival. This is achieved through its interactions with super-enhancers, which are regions of chromatin that drive the expression of genes essential for cell identity and function.¹³ Although BRD2 and BRD3 have not been as extensively studied as BRD4, all three proteins are implicated in tumorigenesis and cancer progression, by mechanisms including the regulation of gene transcription, cell cycle control, inflammation, and immune response.¹⁴ By harnessing the PROTAC technology, researchers aim to selectively degrade these proteins, thus offering a novel therapeutic approach to combat cancers driven by BET proteins dysfunction.¹⁵

Polo-like kinase 1 (PLK1) is another famous oncoprotein closely linked to various cancers.¹⁶ Its abnormal expression is associated with the onset and progression of various cancers, making it a critical target for drug development. Several PLK1 inhibitors have been developed and promoted to clinical trials.¹⁷ Considering the importance of BET and PLK1 in oncogenesis, the dual targeting them by one PROTAC molecule might achieve an enhanced anticancer efficacy.¹⁸ This improved activity can be attributed to the compound's unique ability to engage with two distinct oncogenic pathways simultaneously. Numerous studies have reported that the PLK1 inhibitor BI-2536 is a dual inhibitor of BRD4 and PLK1.¹⁹ which might be utilized as warhead for constructing dual targeting PROTACs (Fig. 1). Previous studies have demonstrated that the dual BET/PLK1 inhibitors could be developed into potent PROTAC molecules for prostate cancer and acute myeloid leukemia therapy.^{20–22} In this study, we designed a series of PROTAC by pairing BI-2536 with cereblon (CRBN) or von Hippel-Lindau (VHL) ligands by aliphatic linkers of variable length. Among these degraders, the 17b compounds showed remarkable efficacy.²³ They not only inhibited the growth of various malignant cancer cells but also induced efficient degradation of both BET proteins and PLK1 kinase, even at low nanomolar concentrations. This approach underscores the potential of dual targeting PROTAC technology, which may benefit anticancer chemotherapy in the future.

2. Results and discussion

2.1. Synthesis of PROTAC based on BI-2536

To achieve the dual degradation of PLK1 kinase and BRD4 bromodomain, we selected BI-2536 as the warhead. BI-2536 exhibits potent inhibitory activity against both BRD4 ($IC_{50} = 0.83$ nM) and PLK1 ($IC_{50} = 25$ nM) according to previous reports.^{24–25} We expected to proteolyze both targets by conjugating BI-2536 with an E3 ligand. Following the aforementioned design principles, we combined BI-2536 with two E3 ubiquitin ligase ligands: Pomalidomide (as a CRBN ligand) and S,R,S-AHPC (as a VHL ligand), using alkyl chains of different lengths as linkers. According to the crystal structures reported by Ding lab²⁶ and Knapp lab,²⁷ the piperidine ring of BI-2536 extrudes outside of the binding pockets when BI-2536 associates with both PLK1 and BRD4 (Fig. 1A). It is postulated that conjugation at the piperidine ring would minimize the risk of disturbing the binding configuration. In our design, we retained the rightmost piperidine ring of BI-2536 and employed a nucleophilic substitution reaction to attach alkyl chain linkers of varying lengths on the nitrogen atom of the piperidine ring. The resulting BI-2536 analogs were then conjugated with either S,R,S-AHPC or pomalidomide (POM) for E3 ligase recruitment. Our hypothesis centers on the linker length, as well as the selection of appropriate E3 ligands, to achieve a potent target degradation (Fig. 1). We posited that these structural elements are critical to determining the potency and selectivity of our dual-targeting PROTACs.²⁸

We designed seven PROTAC compounds and synthesized according to the routes in scheme 1 and scheme 2. Briefly, BI-2536's analog 11 was synthesized from starting material 1 by stepwise condensation of building blocks. The condensing methods used in Scheme 1 were modified from the previous report.²⁹ The BI-2536 analog, compound 11, contains a piperidine group that could readily conjugate with the E3 ligase ligand. In this study, we inserted a fatty acid linker between the compound 11 and E3 ligand to provide flexibility for the formation of the ternary complex.

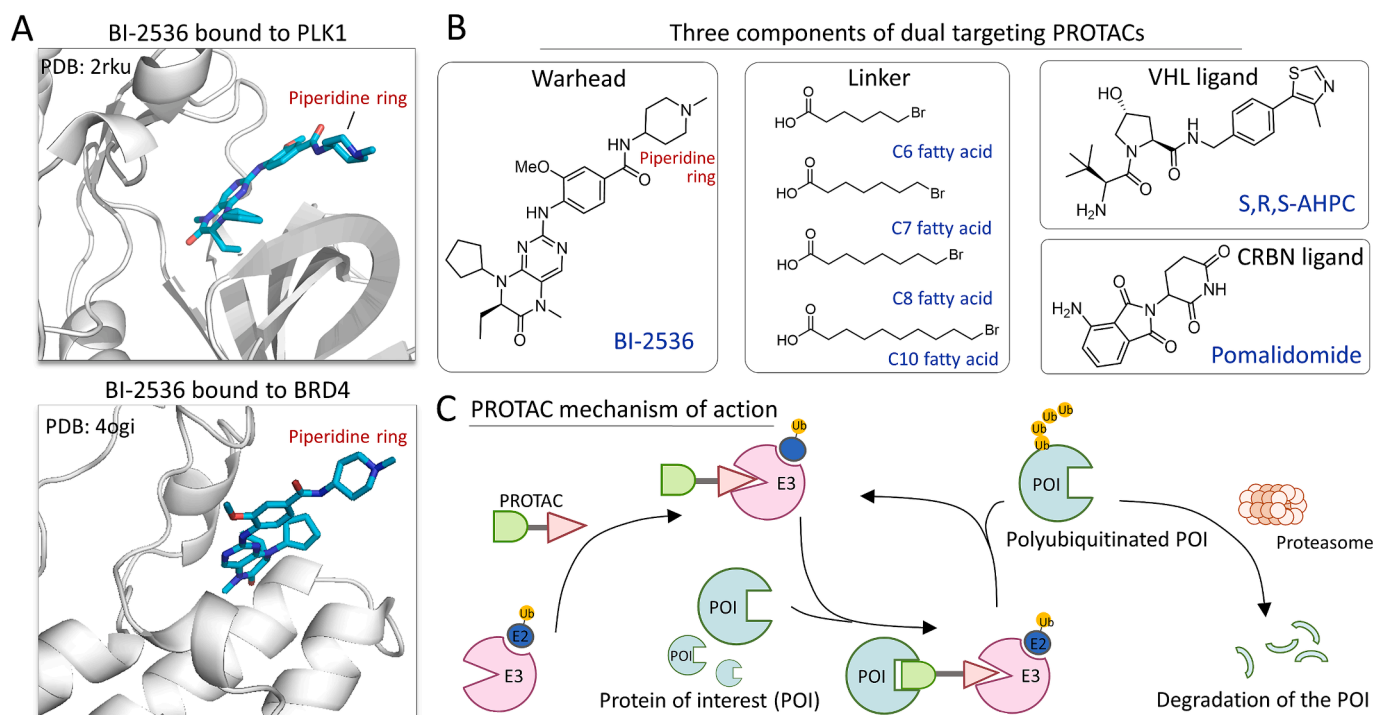
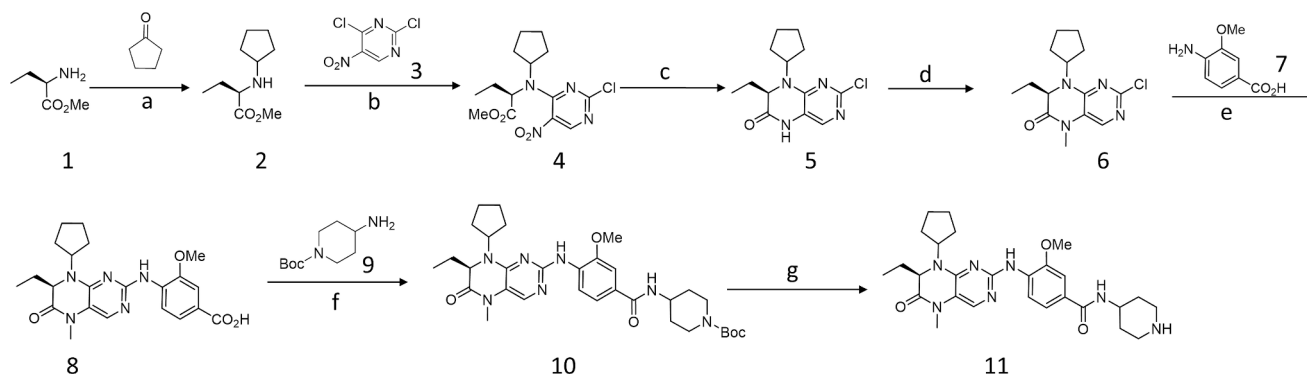
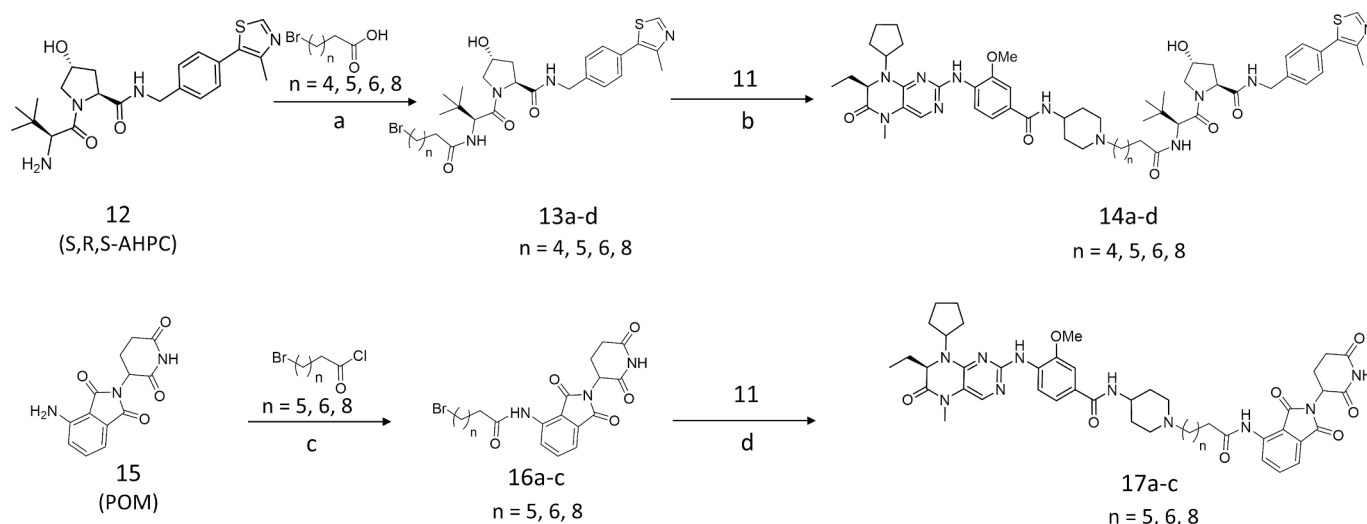


Fig. 1. Scheme illustrating the design of dual targeting PROTAC from BI-2536. (A) Crystal structures of BI-2536 bound to PLK1 (PDB ID: 2rku) and BRD4 (PDB ID: 4ogi). The structural images were visualized and generated by PyMOL (Schrodinger, Inc.). (B) The PROTAC is comprised by BI-2536 (warhead), a fatty acid linker (linker) and E3 ubiquitin ligase (VHL or CRBN) ligands to achieve the dual targeting to PLK1 and BRD4 simultaneously. (C) The mechanism of action of PROTAC.



Scheme 1. Synthetic route of the BI-2536 analog (compound 11). Reagents and conditions: (a) cyclopentanone, NaOAc, NaBHOAc, DCM, 0 °C- r.t., 12 h; (b) NaHCO₃, cyclohexane, 60 °C, 12 h; (c) iron powder, acetic acid, 70 °C – 100 °C, 1.5 h; (d) MeI, NaH, DMF, 0 °C, – r.t., 50 min; (e) HCl, EtOH/H₂O, 90 °C, 24 h; (f) HATU, DIEA, DMF, r.t., 2 h; (g) TFA, DCM, 2 h.



Scheme 2. Synthesis of PROTAC compounds 14a-d and 17a-c. Reagents and conditions: (a) HATU, DIEA, DMF, r.t., 1 h; (b) K₂CO₃, DMF, 60 °C, 3 h; (c) THF, 72 °C, 3 h; (d) K₂CO₃, DMF, 60 °C, 3 h.

According to [Scheme 2](#), we first coupled the VHL ligand S,R,S-AHPC with bromo-substituted fatty acids of variable length by HATU - reagent. The resulting intermediates (compounds 14a-d) contain an alkyl bromide terminal, which is nucleophilically attacked by the piperidine's amine in compound 11. The alkylation reaction underwent smoothly in the presence of base K₂CO₃ at 60 °C, which yielded the PROTAC compounds 14a-d in moderate yields. The POM-based PROTAC molecules 17a-c were synthesized in a similar method. Briefly, compounds 16a-c were generated by coupling POM (15) with the bromo fatty acid chloride despite the weak reactivity of the phenylamine group in POM. The PROTAC 17a-c were finally obtained by alkylation of 11 with 16a-c using the condition above. As confirmed by Nuclear magnetic resonance (NMR) and high-resolution mass spectrometry (HRMS), all the PROTAC molecules are accurate in structure and molecule weight, and ready for biological tests.

2.2. Cytotoxic potency of PROTACs is determined by linker length and E3 ligand

The growth inhibitory effects of these compounds were evaluated on four cancer cells using cell counting kit-8 (CCK-8) cytotoxicity assay. When S,R,S-AHPC was used as the E3 ligand, the inhibitory effects of compounds 14a-14c on K562 cell growth were barely impressive, with IC₅₀ values ranging from 527 nM to 1321 nM. However, the extension of linker length (compound 14d, n = 8) improved the anti-proliferative

activity on K562 cells with an IC₅₀ of 66 nM. A similar trend was also observed on the other 3 cancer cell lines, but they showed different sensitivity to these compounds. In the context of the POM-based PROTACs, the compounds 17b achieved the best IC₅₀ values of 52 nM (K562 cells), which are much lower than its analog 17a (IC₅₀ = 89 ± 1.0 nM) and 17c (IC₅₀ = 133 ± 8 nM). The potency was persistent in all other two cell lines (HeLa and 22Rv1), with the exception of MDA-MB-231 cells (IC₅₀ = 274 ± 1.1 nM). These results demonstrated that POM might be a better E3 ligase recruiter when designing dual-targeting PROTAC molecules using BI-2536.

It is interesting to find that 17b, as the best lead of 7 candidates, shows much less potency than BI-2536, which has IC₅₀ value as low as 0.5 nM on K562 and HeLa cells. The cytotoxic disparity of the two compounds is likely attributed to the difference in mechanism of cell killing, in which BI-2536 blocks the protein bioactivities by inhibition while as 17b likely induced the degradation of target proteins. The difference in mechanism of action may lead to the disparity of cell response after treatment. For example, the inhibitory IC₅₀ of BI-2536 to BRD4 protein is as low as 0.83 nM; while the degradation of BRD4 (DC₅₀) by its PROTAC analog 17b might require a much higher concentration. However, the strong inhibition to target does not mean an advantage over the less potent PROTAC in target degradation. The reason is that BRD4 is not only an atypical kinase that can be inhibited by small molecule but also function as scaffolds for transcriptional regulators and chromatin modulators.³⁰ Degradation of BRD4 by

PROTAC can mitigate both the kinase activity and regulatory functions, which might potentiate the anti-cancer activity in cell lines of certain genetic background. This hypothesis was proved by the observation that 17b exhibited significantly high activity against 22Rv1 cells, despite that BI-2536 is ineffective to inhibit the growth of 22Rv1 cells (Table 1). The study from Liu group revealed that 22Rv1 is the BRCA1-null cell line with defects in DNA damage response (DDR).³¹ By degradation of BRD4, PROTAC 17b exploits the tumor DNA repair pathway deficiencies to preferentially kill cancer cells 22Rv1.³² This result also indicates that BI-2536-based PROTAC, such as 17b, elicits its bioactivities by targeted proteolysis, but not inhibitory effect on PLK1 kinase or BET bromodomains.³³

Besides the E3 ligase ligand, the linker length plays an important role as well. 'Linker science' extends beyond simply connecting the POI and E3 ligands.³⁴ It plays a vital role in regulating the biological and physicochemical properties of PROTACs, including target selectivity, cooperativity, biodistribution, metabolic stability, membrane permeability, and water solubility. For example, the linker might significantly influence the conformation of PROTACs in solution, which affect the ternary complex formation. As shown in Table 1, we did observe the linker effect on both AHPC-based and POM-based PROTACs. It seems that AHPC-based PROTACs prefer a longer linker, with best length of $n = 8$. POM-based PROTACs, however, demonstrated the best activities when the linker has the middle length ($n = 6$).

2.3. Potent degradation of BET proteins by PROTACs

Encouraged by the promising cytotoxic result on cancer cells, we conducted western blotting experiments to evaluate the degradation potential on PLK1 and BRD4 proteins. Our goal was to figure out the molecular mechanism behind the cellular bioactivity. Given that BI-2536 targets both BRD4 and PLK1, it is essential to determine the specificity of their degradation. We first evaluated the degradation of BRD4 and PLK1 proteins in HeLa cells. All PROTAC molecules were applied on HeLa cells for 12h treatment at concentrations of 500 nM, respectively (Fig. 2A). Consistent with the results in Table 1, western blotting analysis showed that compounds 17a-17c are highly effective in degrading the BRD4 protein. Quantification of blotting images revealed that 17b degraded 94 % of BRD4 in HeLa cells. Both 17a and 17c degraded around 90 % (Fig. 2A and Table 1). In contrast to the potent effect of 17a-c, no significant degradation of BRD4 protein was observed in HeLa cells treated by 14a-14c. However, the compound 14d, which exhibits the best antiproliferative activity in all AHPC-based PROTACs, did induce partial degradation of BRD4 protein, but its potency is uncompetitive to any of 17a-c. Surprisingly, we did not observe any degradation to PLK1 protein by all PROTAC molecules in the western

blotting analysis, despite the fact that BI-2536 is a well-known binder of PLK1 kinase. It has been reported that a high concentration of PROTAC molecules might prevent the formation of ternary complex and compromise the proteolysis activity, known as the hook effect. In order to rule out this likelihood, we then evaluated the concentration-dependent degradation of PLK1 and BRD4 by western blotting, as shown in Fig. 2B. HeLa cells were incubated with 17a-17c for 24 h at concentrations of 200, 100, 50, and 20 nM, respectively. The target protein level of the treated cells was analyzed by western blotting. The images in Fig. 2B revealed that BRD4 could be effectively degraded at a low concentration of 20 nM by all three PROTACs. However, the compound 17b demonstrated the most potent efficacy of all the three compounds.

BRD4, a pivotal member of the bromodomain and extra-terminal (BET) family of proteins, plays a critical role in various cellular processes, including gene transcription and cell cycle regulation.³⁵ In the realm of targeted therapies, the development of BRD4-PROTACs (proteolysis-targeting chimeras) has emerged as a promising approach to modulate the activity of this protein.³⁶ Notably, most BRD4-PROTACs have exhibited superior efficacy against the other members of BET family as well. In another word, the degradation process by BRD4-PROTAC is not limited to BRD4 alone, but also extends to other closely related family members.³⁷ Specifically, the targeted degradation of BRD4 has been observed to trigger a cascade effect, leading to the concomitant degradation of BRD2 and BRD3, two additional members of the BET family. The interconnected nature of BET family proteins and the cascading effects of BRD4 degradation play an active role in the degradation process.³⁸ Understanding the molecular mechanisms might highlight the broad implications and potentials of protein degradation by BRD4-PROTACs.

Therefore, we selected compound 17b to investigate whether it also degrades the other two BET family proteins. HeLa cells were treated by 17b at concentrations ranging from 0.01 to 1000 nM for 36 h and the degradation levels of BET proteins were evaluated by western blotting. As shown in Fig. 3A and B, all three BET proteins (BRD3, BRD3 and BRD4) were almost completely degraded at concentrations as low as 3 nM. Semi-quantification analysis of the western blotting images (Fig. 3C) showed that 17b in HeLa achieved DC_{50} values of 1.03 nM for BRD4, 1.74 nM for BRD3, 6.45 nM for RBD2 and 1.64 nM for PLK1, with corresponding D_{max} values of 93.4 %, 93.3 %, 82.8 %, and 78.6 %, respectively. A similar result was observed when applying 17b on 22Rv1 cells, in which the DC_{50} values for BRD4, BRD3, BRD2 and PLK1 are 1.56 nM, 9.45 nM, 1.63 nM and 4.68 nM, with corresponding D_{max} values of 96.5 %, 89.9 %, 91.5 %, and 78.0 %. The result has meticulously demonstrated significant potency against BET family proteins, highlighting the potential of these molecules as powerful therapeutic

Table 1
Optimization of linker length and composition.

Comps	E3 ligase recruiter	Linker (n)	% degradation (500 nM)		IC ₅₀ (nM)		MDA-MB-231	22RV1
			PLK1 (12 h/36 h)	BRD4 (12 h)	K562	HeLa		
BI-2536	na	na	0/na	0	0.43 ± 0.01	0.51 ± 0.05	47 ± 10	> 1000
14a	(S,R,S)-AHPC	4	0.3/na	7	> 1000	398 ± 114	> 1000	> 1000
14b	(S,R,S)-AHPC	5	0/na	10	> 1000	193 ± 45	> 1000	> 1000
14c	(S,R,S)-AHPC	6	6/na	22	527 ± 111	158 ± 83	> 1000	> 1000
14d	(S,R,S)-AHPC	8	8/na	50	66 ± 14	52 ± 6	928 ± 195	225 ± 56
17a	POM	5	18/na	94	89 ± 14	54 ± 6	489 ± 93	48 ± 23
17b	POM	6	28/92	95	52 ± 5	44 ± 4	274 ± 49.3	45 ± 25
17c	POM	8	7/na	93	133 ± 8	125 ± 11	527 ± 335	63 ± 28

* IC₅₀ values were expressed as mean ± SD (n = 3). The abbreviation na stands for 'not available' in the table.

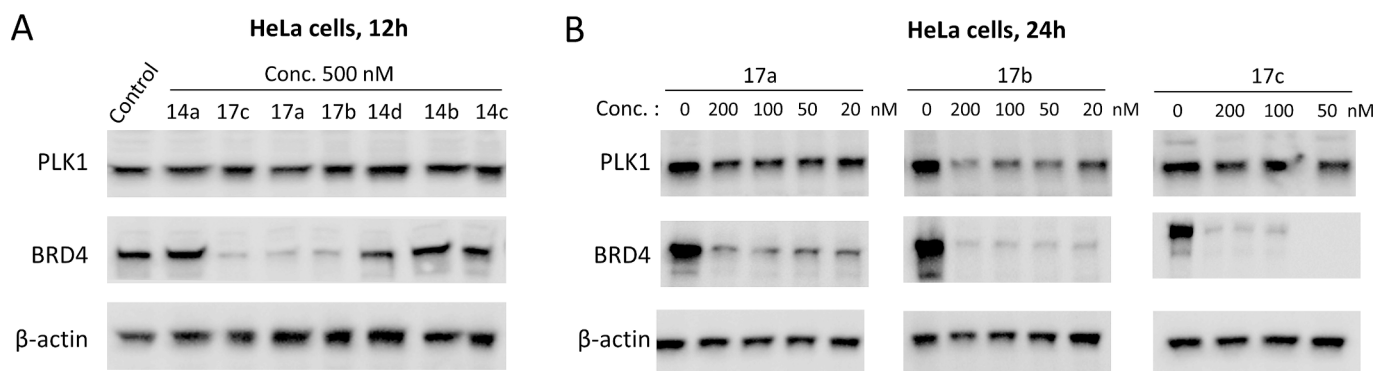


Fig. 2. The screening of PROTAC compounds by western blotting. (A) Western blotting analysis of the PLK1 and BRD4 degradation in HeLa cells after 12 h treatment by various PROTAC compounds (500 nM). (B) Concentration titration of the POM based PROTAC compounds 17a-c in HeLa cells for 24 h treatment.

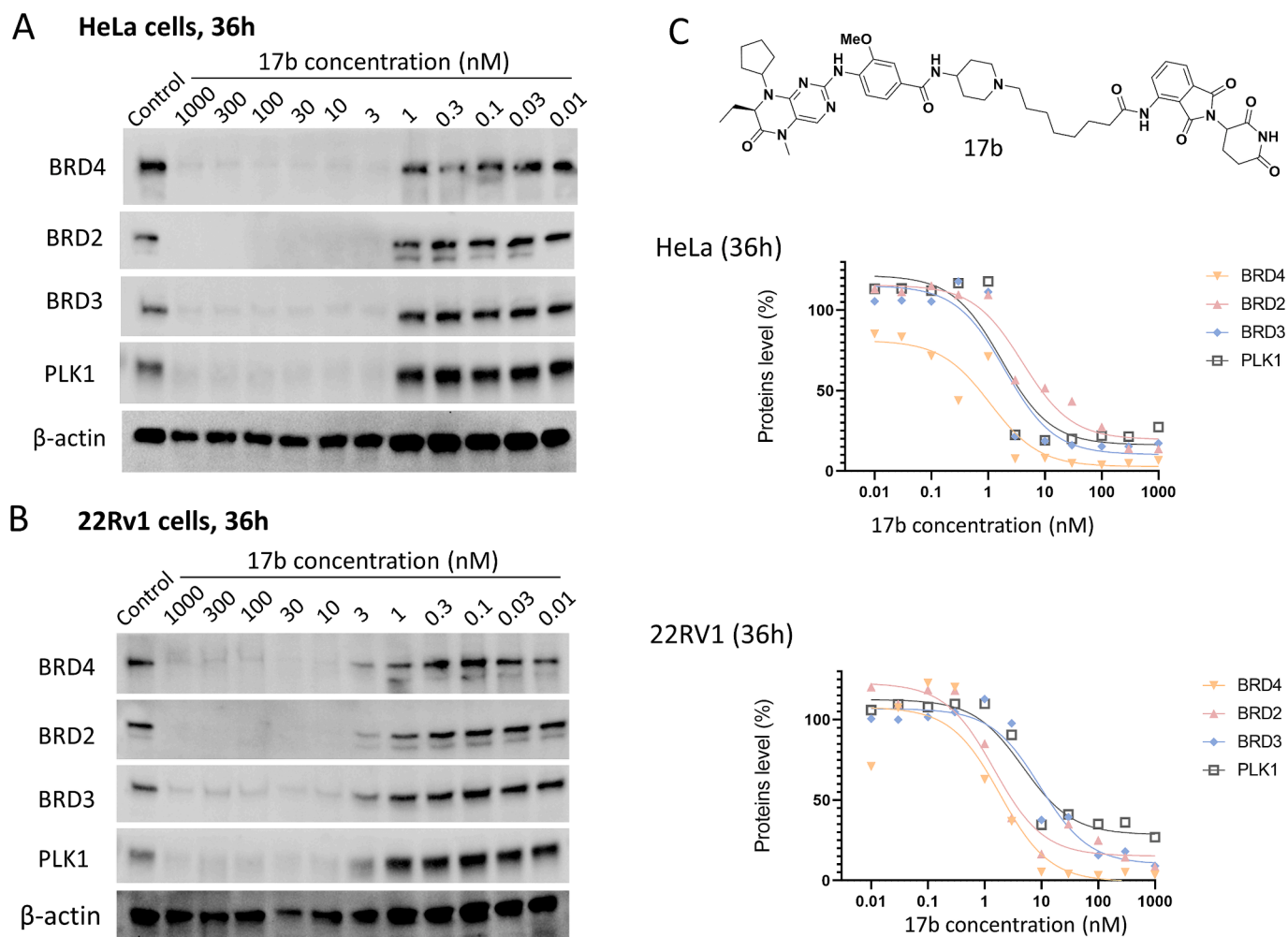


Fig. 3. Further characterization of the lead compound 17b. (A) HeLa Cells were treated with 17b at indicated concentrations for 36 h. The degradation of PLK1 and BET proteins (BRD4, BRD3, BRD2) were examined by western blotting. (B) The target proteins degradation in 22Rv1 cells at the dose ranging from 0.01 to 1000 nM with a 36-h treatment period. (C) Chemical structure of the PROTAC compound 17b, and its proteolysis profiles on HeLa and 22Rv1 cells by quantifying the band intensity from Fig. 3A and 3B.

agents in oncology.

2.4. Time-dependent degradation of PLK1 by PROTAC 17b in cancer cells

It is worth noting that we also observed a moderate proteolysis effect against PLK1 on HeLa cells after 24 h treatment with the high concentration of 17b (200 nM). It is exciting because we did not observe the

degradation of PLK1 at 12 h after treatment even at a much higher concentration of 17b (500 nM), which indicated that the proteolytic targeting of PLK1 is likely time-dependent. Accordingly, we extended the treatment time to 36 h and evaluated the targeted degradation of PLK1 by 17b on two cancer cell lines (HeLa and 22Rv1). The result in Fig. 4A confirmed our hypothesis, as we observed an even higher degradation of PLK1 by 17b at 36 h after treatment. It is worth noting

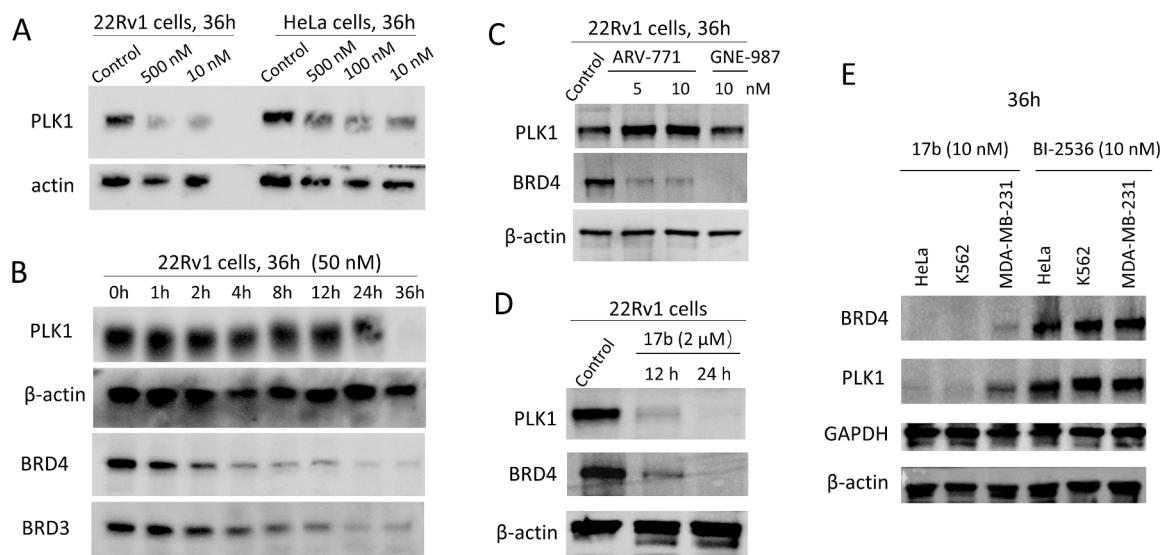


Fig. 4. Time-dependent degradation of PLK1 protein by 17b in 22Rv1 and HeLa cells. (A) The degradation of PLK1 in 22Rv1 and HeLa cells by 17b with a treatment period of 36 h. (B) Time course of target degradation by 17b in 22Rv1 cells (50 nM). (C) The proteolysis of BRD4 and PLK1 by other BRD4-selective PROTACs. (D) Degradation of PLK1 protein by a high concentration of 17b (2 μ M). (E) The proteolysis of targeted proteins in cancer cells after treatment by 17b or BI-2536.

that the additive effect of PLK1 degradation by 17b was negligible during the anti-proliferation assay. It is because that PLK1 degradation by 17b has not transduced to the downstream in the short period of anti-proliferative assay.

We next evaluated the degradation kinetics of 17b on PLK1 and BETs at 50 nM in 22Rv1 cell line (Fig. 4B). Western blot analysis showed that the degradation of PLK1 protein is significantly slower than that of BET family proteins. No significant degradation of PLK1 was observed until 24 h. A profound degradation of PLK1 protein could be detected only 36 h after treatment. It is consistent with our previous experimental conclusions. Western blotting against BRD4 showed that 17b effectively reduced the BRD4 protein level as soon as 2h after treatment, and achieved near-complete depletion of BRD4 proteins 4 h post treatment, indicating a fast kinetics. The degradation of BRD3 is also fast, following a trend similar to that of BRD4 but with a slightly slow kinetic.

The slow degradation of PLK1 by 17b raise a concern about the proteolysis specificity of the PROTAC molecule. To investigate whether the BRD4 pathway crosstalk with PLK1 protein, we analyzed the proteolysis profiles of another two BRD4-selective PROTAC molecules ARV-771 and GNE-987 in 22Rv1 cells. The western blotting images in Fig. 4C reveals that the degradation of BRD4 does not result in downregulation of PLK1 after 36-h treatment, which indicated that PLK1 degradation at 36 h is independent to the BRD4 knockdown. We then increased the 17b concentration during treatment and probed the PLK1 degradation at earlier time points such as 12 h and 24 h (Fig. 4D). Surprisingly, an apparent downregulation of PLK1 was detected, although it is less prominent than that of BRD4. Nevertheless, it proved that PLK1 is targetable by PROTAC molecules but it is less sensitive and speedy. This conclusion is in line with a recent report by Bang group.³⁹ At time point 36 h, the PROTAC 17b is also active in degradation of the dual targets in other cancer cell lines including HeLa, K562 and MDA-MB-231 cell lines (Fig. 4E).

2.5. The downstream pathways and prolonged activity of 17b in cancer cells

The MYC gene, a pivotal member of the proto-oncogene family within the human genome, plays a critical role in cellular regulation. MYC genes encode transcription factors that orchestrate essential biological functions, including cell growth, division, and metabolic homeostasis. The overexpression of the MYC gene is extensively

documented as a significant contributor to the pathogenesis of various human cancers, leading to uncontrolled cell proliferation and resistance to apoptosis. In the pursuit of BRD4-based PROTAC, it has been reported that MYC is one of the critical downstream genes regulated by BRD4.⁴⁰ We examined whether the PROTAC molecule 17b, which induces the degradation of both BET and PLK1, affects the downstream proto-oncogene MYC in cancer cells. To assess this, we employed Real-Time quantitative Polymerase Chain Reaction (RT-qPCR) to measure the mRNA levels of MYC in 17b-treated 22Rv1 cells. The results demonstrated that compound 17b significantly reduced the mRNA levels of MYC in 22Rv1 cells 36 h after treatment (Fig. 5A). Nearly completely down-regulated MYC gene expression could be achieved at a concentration as low as 20 nM, reflecting the potency of 17b to BET proteins.

In an attempt to explore the downstream pathways of PROTAC molecule 17b, we extended our investigation to other genes that might implicate in cell cycle regulation and apoptosis. Specifically, we focused on P21, Bcl-2, PRDM1, and XIAP. Utilizing the RT-qPCR method, we meticulously assessed the mRNA expression patterns of these genes after treatment by compound 17b. Our findings revealed that 17b could downregulate the mRNA expression of numeral genes including Bcl-2, PRDM1, and XIAP (Fig. 5A). This observation is encouraging because all these genes are associated with cell survival and oncogenesis. Moreover, the cyclin-dependent kinase inhibitor P21, a tumor suppressor gene, was unaffected by the treatment of 17b. Collectively, these RT-qPCR results demonstrated that the dual-targeting PROTAC 17b could regulate the downstream genes of BET and PLK1 pathways, reinforcing its molecular mechanism of anticancer effect.

PROTAC molecules usually has a prolonged activity due to the degradation of target proteins. We conduct an in vitro washout experiment to evaluate the long-term anti-proliferation effect of 17b. Briefly, 22Rv1 cells were treated by 17b for 24 h and then continue to be cultured in drug-free media for 1 week. As shown in the Fig. 5B, the anti-proliferative effect was even enhanced when 22Rv1 cells were incubated for 1 week, indicating the long-term activity of 17b.

3. Conclusion

In our efforts to advance targeted cancer therapies, we adopted an approach by combining BI-2536, a well-characterized dual inhibitor of BRD4 and PLK1, with E3 ubiquitin ligase ligand pomalidomide. The combination led to the development of a new class of degraders designed

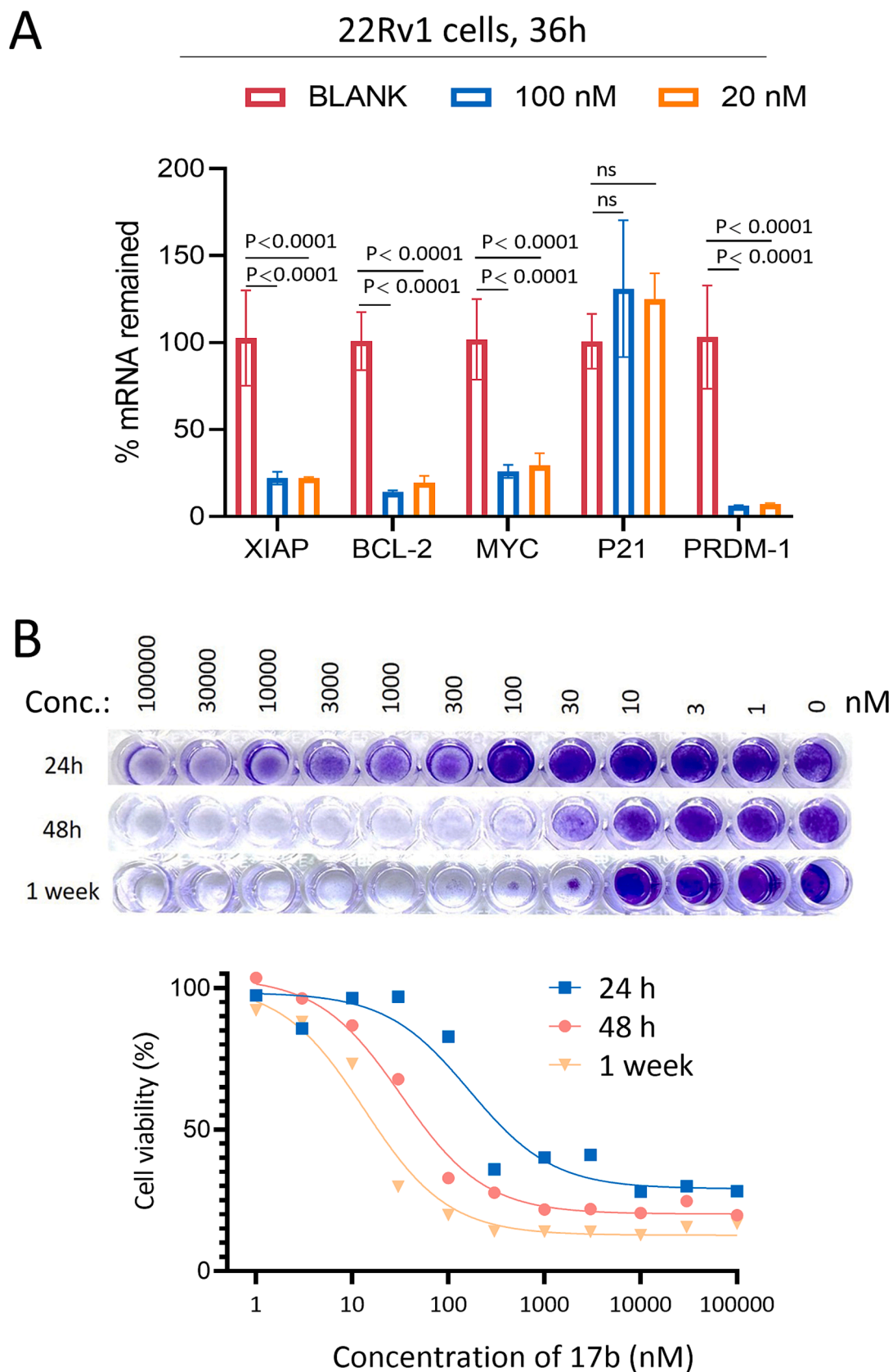


Fig. 5. (A) RT-qPCR analysis of the mRNA levels of 5 genes in 22Rv1 cells following treatment with 17b (20 nM or 100 nM) for 36 h. (B) Cell viability is visualized by crystal violet staining in 22RV1 cells treated with 17b.

to harness the power of targeted protein degradation. We conducted the structural optimization, cytotoxicity screening and target protein degradation evaluation, which finally led to identify 17b as a lead compound from 7 candidates. This compound is a prominent degrader with high specificity to BET and PLK1. However, it elicits the proteolysis of BET protein much faster than that of PLK1. Nevertheless, compound 17b demonstrated strong anti-proliferative activity across a range of cancer cell lines, indicating its therapeutical potentials. Additionally, it exhibits a sustained therapeutic effect in cancer cells, which might be attributed to the catalytic nature of PROTAC molecules. The profound effects in our study suggest that 17b may be a valuable PROTAC molecule with dual targeting capability, showing potential in the targeted cancer chemotherapy.

4. Materials and methods

4.1. Materials and general information

Roswell Park Memorial Institute (RPMI) 1640 medium, Fetal bovine serum (FBS) and other cell culture supplementary reagents were purchased from Procell Inc. (Wuhan, China). Chemicals and solvents were generally purchased from commercial sources (e.g., TCI and bidepharm) and used directly as received without further purification unless otherwise noted. Analytical TLC was conducted on GF254 silica gel plates purchased from Accela ChemBio. Flash column chromatography was performed with silica gel (200–300 mesh) purchased from Accela ChemBio. Nuclear magnetic resonance (NMR) spectra were recorded on Bruker Avance NMR spectrometers operating at 400 MHz or 600 MHz. ¹H NMR chemical shifts were reported in δ units, parts per million (ppm) relative to the chemical shifts of the residual solvent. Reference peaks for DMSO-*d*₆ in ¹H NMR spectra were set at 2.50 ppm, respectively. High-resolution mass spectra (HRMS) were recorded with Thermo Scientific Q Exactive Orbitrap LC-MS system. Low-resolution mass spectra were recorded with Thermo Scientific LCQ Fleet. HPLC analysis was performed with a Shimadzu LC-40 system (Shimadzu, Japan) equipping a WondaSil C18 Superb 5 μ m 4.6 x 150 mm column (GL Sciences). The mobile phase consisted of buffer A (water plus 0.1 % formic acid) and buffer B (acetonitrile plus 0.1 % formic acid) with a flow rate of 1 mL/min and gradient elution for 30 min. The running program is as follows: 95 % buffer A and 5 % buffer B adjust to 5 % buffer A and 95 % buffer B as a gradient from 0 to 20 min, maintain 5 % buffer A and 95 % buffer B from 20 to 25 min, maintain 95 % buffer A and 5 % buffer B from 25 to 30 min.

4.2. Cell lines

HeLa, 22RV1, K562, MDA-MB-231 cells were purchased from American Type Culture Collection (ATCC). Upon thaw, all cells were cultured in Roswell Park Memorial Institute 1640 medium (RPMI 1640, Pricella) supplemented with 10 % fetal bovine serum (FBS, Pricella) and 1 % penicillin–streptomycin (PS, Pricella). All cells were cultured at 37 °C with 5 % CO₂ and regularly checked for the absence of mycoplasma.

4.3. Cell viability and proliferation assay

HeLa, 22RV1, K562, MDA-MB-231 cells (3×10^3 /well) were cultured overnight in 96-well plates. Cells were treated with compounds or DMSO control (Sigma, USA) for 3 days. The living cells in the 96-well plate was counted using a microplate reader using CCK8 (Beyotime, #C0038) reagent. Cell viability and IC₅₀ were profiled using GraphPad Prism 9.4.1.

4.4. Western blotting analysis.

Tumor cells were inoculated in 6-well plates at a density of 2×10^5

cells per well and incubated for 24 h. Following this, cells were treated with either DMSO or specified concentrations of compounds (14a–14d, 17a–17c) for a designated period. After incubation, the culture medium was discarded, and the tumor cells were washed with PBS and lysed with IP buffer (Beyotime P0013). The lysate was centrifuged at 13,000 rpm for 10 min at 4 °C. The supernatant was collected, and protein concentration was determined using a BCA Assay Kit (Thermo A55860). Protein samples (5–20 μ g) were loaded onto a 4–20 % sodium dodecyl sulfate–polyacrylamide gel (ACE Biotechnology ET12420Gel) and subjected to electrophoresis at 120 V for 2.5 h. Proteins were then transferred to an immobilized PVDF membrane (Millipore IPVH00010). The membrane was blocked with 5 % BSA for 1–2 h and incubated with primary antibodies overnight at 4 °C or 1.5 h at room temperature. The membrane was washed 3–4 times with TBST (Tris-buffered saline with Tween 20), each wash lasting 5 min. Following this, the membrane was incubated with HRP-conjugated secondary antibodies at room temperature for 1 h, washed three times with TBST (each wash lasting 8 min), and treated with ECL enhanced HRP substrate (Proteintech PK10001). Chemiluminescence was detected using a ChemiDoc XRS + gel imaging system (Bio-Rad). The primary antibodies used were anti-BRD4 (1:3000 dilution, CST#13440), anti-BRD3 (1:100 dilution, Santa Cruz sc-81202), anti-BRD2 (1:3000 dilution, NatureBios A95996), anti-PLK1 (1:3000 dilution, Invitrogen 37-7000) and anti- β -actin (1:5000 dilution, 81115–1-RR). The secondary antibodies were HRP-conjugated Goat anti-Rabbit IgG (ABclonal, AS014, 1:10000) and HRP-conjugated Goat anti-Mouse IgG (ABclonal, AS003, 1:10000).

4.5. RNA isolation and quantitative RT-PCR analysis

Cells were treated with compound or DMSO for 36 h, and then total RNA was extracted with trizol, according to the manufacturer's instruction. Then, qPCR was performed using the Hiscript II One Step Qrt-PCR SYBR Green Kit (Vazyme) in triplicate on an the CFX Connect RT-qPCR system (BIO-RAD) in accordance with the manufacturer's instruction. The primer pairs used for qPCR were as follows: BCL-2-F: CTGCACCTGACGCCCTTACC, BCL-2-R: CACATGACCCACCGAACTCAAAGA; MYC-F: GGCTCCTGGCAAAGGTC, MYC-R: CTGCGTAGTTGTGCTGATGT; P21-F: TGGAGACTCTCAGGGTCGAA, P21-R: GGATTA-GGGCTTCTCTTGG; XIAP-F: GTGACTAGATCTCCA-CAAG; XIAP-R: GTTCAGGAGTGTCTGGTAAAG; PRDM1-F: GTTCTTAAGAACGCCAACAGG, PRDM1-R: GCAAAGTCCCGACAA-TACCAC; β -actin-F: GAAATCGTGGTGACATCAAAG, β -actin-R: TGTAGTTTCATGGATGCCACAG. All of the gene expressions were determined by normalizing to the levels of the control gene β -actin and calculated by the DDCT method.

4.6. Crystal violet staining experiment

22RV1 cells (1×10^4 cells per well) were cultured overnight in 96-well plates. The cells were then treated with either the compound or DMSO (Sigma USA) for the specified duration. The cells were fixed in a 4 % paraformaldehyde solution and subsequently stained with Crystal Violet Staining Solution (Beyotime, C0121). After thorough washing with PBS, the cells were ready for observation and photography. The eluent was decolorized using 33 % acetic acid and then eluted on a shaker at room temperature for 20 min. The optical density (OD) value of the eluent was subsequently measured at 570 nm using an enzymograph. Cell viability was calculated using GraphPad Prism 9.4.1.

4.7. Chemical synthesis of PROTACs

4.7.1. Methyl (R)-2-(cyclopentylamino) butanoate (2)

Compound 1 (7.4 g) and cyclopentanone (4.1 g, 49 mmol) were dissolved in 80 mL DCM. After the addition of sodium acetate (4.0 g, 4 mmol) and sodium triacetoxyborohydride (15.0 g, 71 mmol) at 0 °C, the reaction was stirred for 12 h at room temperature and then 50 mL

saturated sodium bicarbonate solution were added. The aqueous phase was extracted with dichloromethane. The organic phases were washed with water, dried over MgSO_4 and evaporated down to give (R)-methyl 2-(cyclopentylamino)butanoate as a yellow oil (compound 2, 8.6 g, yield: 95 %). HRMS (ESI) m/z : $[\text{M} + \text{H}]^+$ calculated for $\text{C}_{10}\text{H}_{20}\text{NO}_3$ 186.1494, found 186.1485.

4.7.2. Methyl (R)-2-((2-chloro-5-nitropyrimidin-4-yl) (cyclopentyl) amino) butanoate (4)

Compound 2 (1.25 g, 6.75 mmol) and sodium bicarbonate (4.20 g, 50 mmol) were dissolved in 50 mL of cyclohexane, stirred for 0.5 h followed by the addition of Compound 3 (2.91 g, 15.0 mmol), heated to 60 °C and stirred for 12 h. The reaction mixture was filtered, washed with DCM (50 mL), and the filtrate was concentrated under reduced pressure, the resulting residue was recrystallized by 150 mL of the mixture solvent of ethyl acetate and *n*-hexane (V/V = 1:4) to obtain the title compound 4 (1.70 g, yield: 73 %) as a yellow solid. HRMS (ESI) m/z : $[\text{M} + \text{H}]^+$ calculated for $\text{C}_{14}\text{H}_{20}\text{ClN}_4\text{O}_4$ 343.1173, found 343.1165.

4.7.3. (R)-2-chloro-8-cyclopentyl-7-ethyl-7,8-dihydropteridin-6(5H)-one (5)

To a solution of Compound 4 (300 mg, 0.66 mmol) were dissolved in 1 mL glacial acetic acid and at 70 °C. 40 mg iron powder was added batchwise. The mixture was stirred for 1.5 h at 100 °C. and then filtered hot through kieselguhr. The reaction mixture was evaporated down, taken up in methanol/dichloromethane, applied to silica gel and purified by Soxhlet extraction with ethyl acetate. The solvent was removed and the residue was stirred with methanol. Yield: compound 5 (200 mg, yield: 74 %). ^1H NMR (400 MHz, $\text{DMSO}-d_6$) δ 10.87 (s, 1H), 7.56 (s, 1H), 4.11 (d, $J = 16.5$ Hz, 1H), 2.51 (d, $J = 2.1$ Hz, 1H), 1.98 – 1.64 (m, 8H), 1.53 (s, 2H), 0.77 (t, $J = 7.4$ Hz, 3H). HRMS (ESI) m/z : $[\text{M} + \text{H}]^+$ calculated for $\text{C}_{13}\text{H}_{18}\text{ClN}_4\text{O}$ 281.1169, found, 281.1157.

4.7.4. (R)-2-chloro-8-cyclopentyl-7-ethyl-5-methyl-7,8-dihydropteridin-6(5H)-one (6)

Compound 5 (500 mg, 1.79 mmol) was dissolved in 2 ml of dimethylacetamide before methyl iodide (79 μL , 1.5 mmol) was added. The reaction was cooled down to 0 °C and sodium hydride as a 60 % dispersion in mineral oil (38 mg, 0.95 mmol) was added. The reaction mixture was stirred for 50 min at room temperature. the organic compound taken up into Ethyl acetate and wash with water five times. The organic layer was dried using Na_2SO_4 and organic layer removed under reduced pressure affording compound 6 (250 mg, yield: 47 %) as yellow crystals. ^1H NMR (600 MHz, $\text{DMSO}-d_6$) δ 7.86 (s, 1H), 4.34 (dd, $J = 7.1$, 3.4 Hz, 1H), 4.16 (p, $J = 8.4$ Hz, 1H), 3.24 (s, 3H), 1.96 – 1.88 (m, 2H), 1.87 – 1.77 (m, 5H), 1.70 (dt, $J = 14.3$, 6.7 Hz, 1H), 1.61 – 1.47 (m, 2H), 0.73 (t, $J = 7.5$ Hz, 3H). ^{13}C NMR (151 MHz, $\text{DMSO}-d_6$) δ 163.20, 151.56, 138.52, 121.27, 60.80, 59.36, 28.42, 27.94, 26.65, 23.89, 8.51. HRMS (ESI) m/z : $[\text{M} + \text{H}]^+$ calculated for $\text{C}_{14}\text{H}_{20}\text{ClN}_4\text{O}$ 295.1326, found 295.1312.

4.7.5. (R)-4-((8-cyclopentyl-7-ethyl-5-methyl-6-oxo-5,6,7,8-tetrahydropteridin-2-yl) amino)-3-methoxybenzoic acid (8)

Compound 6 (220 mg, 0.74 mmol) and compound 7 (230 mg, 1.50 mmol) were suspended in 0.3 ml of ethanol, 1.2 ml of water and 130 μL of concentrated hydrochloric acid and at 90 °C for 24h. Volatiles were evaporated under reduced pressure and the residue stirred with methanol/diethyl ether and the precipitate formed was filtered affording compound 8 (158 mg, yield: 50 %) as a white solid. ^1H NMR (600 MHz, $\text{DMSO}-d_6$) δ 9.80 (s, 1H), 7.99 – 7.86 (m, 2H), 7.67 – 7.53 (m, 2H), 4.49 (dd, $J = 6.5$, 3.2 Hz, 1H), 4.17 (p, $J = 9.3$ Hz, 1H), 3.90 (s, 3H), 3.22 (s, 3H), 1.99 – 1.87 (m, 3H), 1.80 (dq, $J = 14.4$, 7.0 Hz, 3H), 1.55 – 1.39 (m, 4H), 0.74 (t, $J = 7.4$ Hz, 3H). ^{13}C NMR (151 MHz, $\text{DMSO}-d_6$) δ 162.46, 152.28, 150.35, 148.83, 130.02, 127.51, 121.90, 115.88, 111.68, 61.19, 55.98, 28.22, 27.81, 26.93, 22.85, 8.02. HRMS (ESI) m/z : $[\text{M} + \text{H}]^+$ calculated for $\text{C}_{22}\text{H}_{28}\text{N}_5\text{O}_4$ 426.2141, found 426.2133.

4.7.6. Tert-butyl (R)-4-((8-cyclopentyl-7-ethyl-5-methyl-6-oxo-5,6,7,8-tetrahydropteridin-2-yl) amino)-methoxybenzamido)piperidine-1-carboxylate (10)

To a solution of Compound 8 (100 mg, 0.22 mmol) in DMF (2 mL) were added Compound 9 (57 mg, 0.29 mmol), HATU (167 mg, 0.44 mmol) and DIPEA (53 mg, 0.44 mmol). After being stirred at room temperature for 2h, The organic layer was concentrated under reduced pressure. The crude residue was purified by flash column chromatography with DCM/MeOH (20:1) to obtain a compound 10 (100 mg, yield: 72 %). ^1H NMR (400 MHz, $\text{DMSO}-d_6$) δ 8.42 (d, $J = 8.9$ Hz, 1H), 8.11 (d, $J = 7.9$ Hz, 1H), 7.85 (s, 1H), 7.61 (s, 1H), 7.47 (d, $J = 7.1$ Hz, 2H), 4.41 – 4.30 (m, 1H), 4.29 – 4.21 (m, 1H), 3.98 (d, $J = 7.3$ Hz, 3H), 3.93 (s, 3H), 3.24 (s, 3H), 2.84 (d, $J = 20.6$ Hz, 3H), 2.01 (d, $J = 7.2$ Hz, 1H), 1.88 (d, $J = 6.8$ Hz, 2H), 1.83 – 1.67 (m, 6H), 1.67 – 1.53 (m, 3H), 1.41 (s, 10H), 0.76 (t, $J = 7.4$ Hz, 3H). ^{13}C NMR (151 MHz, $\text{DMSO}-d_6$) δ 164.89, 162.77, 153.98, 152.07, 119.96, 116.01, 109.96, 78.77, 53.66, 48.81, 46.71, 28.17, 26.90, 23.11, 18.13, 16.78, 8.44. HRMS (ESI) m/z : $[\text{M} + \text{H}]^+$ calculated for $\text{C}_{32}\text{H}_{46}\text{N}_7\text{O}_5$ 608.3560, found 608.3552.

4.7.7. Tert-butyl (R)-4-((8-cyclopentyl-7-ethyl-5-methyl-6-oxo-5,6,7,8-tetrahydropteridin-2-yl) amino)-3-methoxy-N-(piperidin-4-yl)benzamide (11)

To a solution of Compound 10 (95 mg, 0.15 mmol) in DCM (2 mL) were added TFA (1 mL). After being stirred at room temperature for 2h. The resulting mixture was concentrated to afford the compound 11 as crude colorless oil (70 mg). ^1H NMR (600 MHz, $\text{DMSO}-d_6$) δ 8.42 (d, $J = 8.4$ Hz, 1H), 8.30 (d, $J = 7.4$ Hz, 1H), 7.84 (s, 1H), 7.64 (s, 1H), 7.53 – 7.44 (m, 2H), 4.38 – 4.29 (m, 1H), 4.24 (d, $J = 3.5$ Hz, 1H), 4.13 – 4.02 (m, 1H), 3.94 (s, 3H), 3.33 (s, 2H), 3.24 (s, 3H), 3.03 (t, $J = 11.8$ Hz, 2H), 2.54 (s, 1H), 2.05 – 1.96 (m, 3H), 1.90 (d, $J = 23.6$ Hz, 2H), 1.83 – 1.67 (m, 6H), 1.62 (dq, $J = 21.0$, 7.2 Hz, 3H), 0.76 (t, $J = 7.5$ Hz, 3H). ^{13}C NMR (151 MHz, $\text{DMSO}-d_6$) δ 165.53, 162.99, 154.29, 151.56, 146.74, 132.36, 126.40, 120.32, 116.19, 109.33, 58.36, 56.10, 44.51, 42.52, 28.80, 28.49, 27.86, 26.54. HRMS (ESI) m/z : $[\text{M} + \text{H}]^+$ calculated for $\text{C}_{27}\text{H}_{38}\text{N}_7\text{O}_3$ 508.3036, found 508.3025.

4.7.8. (2S,4R)-1-((S)-2-(6-bromohexanamido)-3,3-dimethylbutanoyl)-4-hydroxy-N-(4-(4-methylthiazol-5-yl)benzyl)pyrrolidine-2-carboxamide (13a)

To a solution of Compound 12 (40 mg, 0.09 mmol) in DMF (2 mL) were added compound 6-bromohexanoic acid (25 mg, 0.12 mmol), HATU (68 mg, 0.18 mmol) and DIPEA (21 mg, 0.18 mmol). After being stirred at room temperature for 1 h, The organic layer was concentrated under reduced pressure. The crude residue was purified by flash column chromatography with DCM/MeOH (20:1) to obtain a white solid (40 mg, yield: 71 %). ^1H NMR (400 MHz, $\text{DMSO}-d_6$) δ 8.99 (s, 1H), 8.59 (t, $J = 6.0$ Hz, 1H), 7.91 (d, $J = 9.4$ Hz, 1H), 7.40 (q, $J = 8.4$ Hz, 4H), 5.15 (d, $J = 3.0$ Hz, 1H), 4.54 (d, $J = 9.4$ Hz, 1H), 4.50 – 4.39 (m, 2H), 4.34 (s, 1H), 4.23 (d, $J = 5.5$ Hz, 1H), 3.65 (d, $J = 4.2$ Hz, 2H), 3.50 (d, $J = 6.7$ Hz, 2H), 2.44 (s, 3H), 2.26 (dt, $J = 14.8$, 7.6 Hz, 1H), 2.13 (dt, $J = 14.2$, 7.1 Hz, 1H), 2.06 – 1.99 (m, 1H), 1.90 (td, $J = 8.5$, 4.4 Hz, 1H), 1.78 (q, $J = 7.1$ Hz, 2H), 1.50 (dq, $J = 14.7$, 7.6 Hz, 2H), 1.41 – 1.29 (m, 2H), 0.93 (s, 9H). ^{13}C NMR (151 MHz, $\text{DMSO}-d_6$) δ 171.97, 151.49, 147.73, 131.19, 128.66, 127.44, 68.88, 58.70, 56.37, 41.66, 37.97, 35.23, 35.11, 34.67, 31.95, 27.22, 26.41, 24.56, 15.96. ESI $m/z = 607.32$ $[\text{M} + \text{H}]^+$.

4.7.9. (2S,4R)-1-((S)-2-(7-bromoheptanamido)-3,3-dimethylbutanoyl)-4-hydroxy-N-(4-(4-methylthiazol-5-yl)benzyl)pyrrolidine-2-carboxamide (13b)

Compound 13b (32 mg, yield: 56 %) was obtained as a yellow powder using the procedure employed for the synthesis of compound 13a. ^1H NMR (400 MHz, $\text{DMSO}-d_6$) δ 8.99 (s, 1H), 8.58 (t, $J = 6.0$ Hz, 1H), 7.89 (d, $J = 9.4$ Hz, 1H), 7.40 (q, $J = 8.3$ Hz, 4H), 5.14 (d, $J = 3.5$ Hz, 1H), 4.54 (d, $J = 9.4$ Hz, 1H), 4.48 – 4.39 (m, 2H), 4.34 (s, 1H), 4.21 (dd, $J = 15.9$, 5.5 Hz, 1H), 3.69 – 3.62 (m, 2H), 3.51 (t, $J = 6.7$ Hz, 2H),

2.44 (s, 3H), 2.25 (dd, $J = 14.3, 7.2$ Hz, 1H), 2.12 (dt, $J = 14.2, 7.1$ Hz, 1H), 2.06–1.98 (m, 1H), 1.89 (ddd, $J = 12.9, 8.6, 4.6$ Hz, 1H), 1.77 (p, $J = 6.9$ Hz, 2H), 1.48 (dq, $J = 17.6, 6.7$ Hz, 2H), 1.40–1.31 (m, 2H), 1.26 (q, $J = 7.2$ Hz, 2H), 0.93 (s, 9H). ^{13}C NMR (151 MHz, DMSO- d_6) δ 172.22, 172.07, 169.79, 151.56, 147.79, 139.56, 129.70, 128.72, 127.50, 68.95, 58.78, 56.42, 41.73, 38.00, 35.29, 35.23, 32.19, 27.79, 27.30, 26.45, 25.31, 16.01. ESI $m/z = 621.04$ [M + H] $^+$.

4.7.10. (2S,4R)-1-((S)-2-(8-bromooctanamido)-3,3-dimethylbutanoyl)-4-hydroxy-N-(4-(4-methylthiazol-5-yl)benzyl)pyrrolidine-2-carboxamide (13c)

Compound 13c (30 mg, yield: 50 %) was obtained as a yellow powder using the procedure employed for the synthesis of compound 13a. ^1H NMR (400 MHz, DMSO- d_6) δ 8.99 (s, 1H), 8.59 (t, $J = 6.0$ Hz, 1H), 7.88 (d, $J = 9.4$ Hz, 1H), 7.40 (q, $J = 8.3$ Hz, 4H), 5.14 (d, $J = 3.5$ Hz, 1H), 4.54 (d, $J = 9.4$ Hz, 1H), 4.43 (dt, $J = 12.3, 7.1$ Hz, 2H), 4.34 (s, 1H), 4.21 (dd, $J = 15.9, 5.4$ Hz, 1H), 3.65 (d, $J = 5.6$ Hz, 2H), 3.52 (t, $J = 6.7$ Hz, 2H), 2.44 (s, 3H), 2.25 (dd, $J = 14.5, 7.3$ Hz, 1H), 2.16–2.07 (m, 1H), 2.04 (dd, $J = 20.3, 7.7$ Hz, 1H), 1.94–1.85 (m, 1H), 1.77 (p, $J = 6.7$ Hz, 2H), 1.47 (tt, $J = 13.8, 6.9$ Hz, 2H), 1.34 (d, $J = 7.2$ Hz, 2H), 1.25 (s, 4H), 0.93 (s, 9H). ^{13}C NMR (151 MHz, DMSO- d_6) δ 174.62, 172.26, 172.07, 151.55, 147.79, 128.72, 127.50, 68.95, 58.78, 56.43, 41.73, 38.01, 35.30, 34.88, 33.68, 32.27, 28.52, 28.43, 27.86, 27.49, 27.44, 26.45, 25.39, 24.45, 16.01. ESI $m/z = 635.42$ [M + H] $^+$.

4.7.11. (2S,4R)-1-((S)-2-(10-bromodecanamido)-3,3-dimethylbutanoyl)-4-hydroxy-N-(4-(4-methylthiazol-5-yl)benzyl)pyrrolidine-2-carboxamide (13d)

Compound 13d (30 mg, yield: 50 %) was obtained as a yellow powder using the procedure employed for the synthesis of compound 13a. ^1H NMR (400 MHz, DMSO- d_6) δ 8.98 (s, 1H), 8.58 (t, $J = 6.1$ Hz, 1H), 7.87 (d, $J = 9.3$ Hz, 1H), 7.40 (q, $J = 8.3$ Hz, 4H), 5.14 (d, $J = 3.4$ Hz, 1H), 4.54 (d, $J = 9.4$ Hz, 1H), 4.48–4.38 (m, 2H), 4.38–4.31 (m, 1H), 4.20 (dd, $J = 15.9, 5.5$ Hz, 1H), 3.70–3.61 (m, 2H), 3.51 (t, $J = 6.7$ Hz, 2H), 2.44 (s, 3H), 2.25 (dt, $J = 14.8, 7.7$ Hz, 1H), 2.09 (ddd, $J = 14.4, 8.1, 6.3$ Hz, 1H), 2.05–1.97 (m, 1H), 1.89 (ddd, $J = 12.9, 8.7, 4.6$ Hz, 1H), 1.77 (p, $J = 6.9$ Hz, 2H), 1.47 (dq, $J = 14.1, 6.7$ Hz, 2H), 1.35 (q, $J = 6.9$ Hz, 2H), 1.23 (s, 8H), 0.93 (s, 9H). ^{13}C NMR (151 MHz, DMSO- d_6) δ 172.67, 172.46, 151.93, 131.65, 129.11, 127.89, 69.34, 59.17, 56.81, 42.12, 38.39, 35.68, 35.33, 32.70, 29.25, 29.06, 28.52, 27.96, 26.83, 16.39. ESI $m/z = 663.48$ [M + H] $^+$.

4.7.12. (2S,4R)-1-((S)-2-(6-(4-(4-((R)-8-cyclopentyl-7-ethyl-5-methyl-6-oxo-5,6,7,8-tetrahydropteridin-2-yl)amino)-3-methoxybenzamido) piperidin-1-yl)hexanamido)-3,3-dimethylbutanoyl)-4-hydroxy-N-(4-(4-methylthiazol-5-yl)benzyl)pyrrolidine-2-carboxamide (14a)

To a solution of compound 13a (20 mg, 0.033 mmol) and Compound 11 (24 mg, 0.047 mmol) in DMF were added K_2CO_3 (8 mg, 0.06 mmol), the reaction mixture was then stirred at 60 °C for 3 h. The resulting mixture was purified by preparative HPLC (5 %–100 % acetonitrile plus 0.1 % formic acid / 0.1 % water plus 0.1 % formic acid). The product containing fractions were concentrated to remove the organic solvent under reduced pressure and then dried by lyophilization to afford compound 14a as white solid (20 mg, yield: 58 %). ^1H NMR (600 MHz, DMSO- d_6) δ 8.98 (s, 1H), 8.57 (t, $J = 6.1$ Hz, 1H), 8.42 (d, $J = 8.3$ Hz, 1H), 8.18 (s, 1H), 8.16 (d, $J = 7.5$ Hz, 1H), 7.89–7.82 (m, 2H), 7.61 (s, 1H), 7.48 (d, $J = 9.6$ Hz, 2H), 7.42 (d, $J = 8.3$ Hz, 2H), 7.38 (d, $J = 8.3$ Hz, 2H), 5.14 (s, 1H), 4.55 (d, $J = 9.4$ Hz, 1H), 4.46–4.40 (m, 2H), 4.36 (d, $J = 6.2$ Hz, 2H), 4.23 (dd, $J = 7.4, 3.5$ Hz, 2H), 3.94 (s, 3H), 3.88 (d, $J = 3.8$ Hz, 1H), 3.69–3.61 (m, 3H), 3.24 (s, 3H), 3.12 (d, $J = 9.6$ Hz, 2H), 2.56 (s, 2H), 2.44 (s, 3H), 2.28 (dt, $J = 14.6, 7.6$ Hz, 1H), 2.14 (dt, $J = 14.2, 7.2$ Hz, 1H), 2.08–1.97 (m, 2H), 1.94–1.83 (m, 5H), 1.76 (dd, $J = 12.6, 5.4$ Hz, 4H), 1.72–1.55 (m, 6H), 1.54 (d, $J = 6.9$ Hz, 4H), 1.27 (d, $J = 7.5$ Hz, 2H), 0.94 (s, 9H), 0.76 (t, $J = 7.5$ Hz, 3H). ^{13}C NMR (151 MHz, DMSO- d_6) δ 171.99, 171.95, 163.50, 162.94, 154.32, 151.51, 151.46, 147.73, 139.52, 138.32, 129.65, 128.65, 127.43, 120.17,

115.93, 109.26, 68.88, 59.76, 58.71, 58.30, 56.30, 56.06, 51.69, 41.66, 37.99, 35.26, 34.72, 28.77, 28.48, 27.81, 26.48, 26.40, 26.29, 25.20, 25.05, 23.28, 23.00, 15.96, 8.88. HRMS (ESI) m/z : [M + H] $^+$ calculated for $\text{C}_{55}\text{H}_{76}\text{N}_{11}\text{O}_7\text{S}$ 1034.5650, found 1034.5637. HPLC (purity): 98.95 % ($\lambda = 254$ nm, $t_{\text{R}} = 11.885$ min).

4.7.13. (2S,4R)-1-((S)-2-(7-(4-(4-((R)-8-cyclopentyl-7-ethyl-5-methyl-6-oxo-5,6,7,8-tetrahydropteridin-2-yl)amino)-3-methoxybenzamido) piperidin-1-yl)heptanamido)-3,3-dimethylbutanoyl)-4-hydroxy-N-(4-(4-methylthiazol-5-yl)benzyl)pyrrolidine-2-carboxamide (14b)

Compound 14b (20 mg, yield: 60 %) was obtained as a yellow powder using the procedure employed for the synthesis of compound 14a. ^1H NMR (600 MHz, DMSO- d_6) δ 8.98 (s, 1H), 8.57 (t, $J = 6.0$ Hz, 1H), 8.42 (d, $J = 8.3$ Hz, 1H), 8.21 (s, 1H), 8.16 (d, $J = 7.5$ Hz, 1H), 7.88–7.81 (m, 2H), 7.60 (s, 1H), 7.48 (s, 2H), 7.42 (d, $J = 8.2$ Hz, 2H), 7.38 (d, $J = 8.3$ Hz, 2H), 4.55 (d, $J = 9.4$ Hz, 1H), 4.47–4.41 (m, 2H), 4.38–4.33 (m, 2H), 4.25–4.19 (m, 2H), 3.93 (s, 3H), 3.90–3.86 (m, 1H), 3.72–3.61 (m, 3H), 3.24 (s, 3H), 3.11 (d, $J = 11.0$ Hz, 2H), 2.58–2.53 (m, 2H), 2.44 (s, 3H), 2.27 (dt, $J = 14.8, 7.7$ Hz, 1H), 2.13 (dt, $J = 14.3, 7.3$ Hz, 1H), 2.08–1.99 (m, 2H), 1.94–1.83 (m, 5H), 1.81–1.74 (m, 4H), 1.74–1.54 (m, 6H), 1.49 (s, 4H), 1.26 (s, 4H), 0.94 (s, 9H), 0.76 (t, $J = 7.5$ Hz, 3H). ^{13}C NMR (151 MHz, DMSO- d_6) δ 171.97, 165.34, 163.78, 151.46, 138.32, 128.65, 127.44, 120.18, 115.92, 109.25, 68.89, 59.77, 58.72, 58.31, 56.38, 56.31, 51.69, 41.67, 39.10, 37.99, 35.25, 34.82, 30.39, 28.78, 27.81, 26.49, 26.41, 25.21, 23.27, 23.00, 15.96, 8.88. HRMS (ESI) m/z : [M + H] $^+$ calculated for $\text{C}_{57}\text{H}_{78}\text{N}_{11}\text{O}_7\text{S}$ 1048.5806, found 1048.5775. HPLC (purity): 98.84 % ($\lambda = 254$ nm, $t_{\text{R}} = 12.290$ min).

4.7.14. (2S,4R)-1-((S)-2-(8-(4-(4-((R)-8-cyclopentyl-7-ethyl-5-methyl-6-oxo-5,6,7,8-tetrahydropteridin-2-yl)amino)-3-methoxybenzamido) piperidin-1-yl)octanamido)-3,3-dimethylbutanoyl)-4-hydroxy-N-(4-(4-methylthiazol-5-yl)benzyl)pyrrolidine-2-carboxamide (14c)

Compound 14c (15 mg, yield: 45 %) was obtained as a yellow powder using the procedure employed for the synthesis of compound 14a. ^1H NMR (600 MHz, DMSO- d_6) δ 8.98 (s, 1H), 8.59 (t, $J = 6.1$ Hz, 1H), 8.42 (s, 1H), 8.34 (d, $J = 6.7$ Hz, 1H), 8.15 (s, 1H), 7.88–7.82 (m, 2H), 7.62 (s, 1H), 7.52 (d, $J = 9.7$ Hz, 2H), 7.42 (d, $J = 8.2$ Hz, 2H), 7.38 (d, $J = 8.2$ Hz, 2H), 5.16 (s, 1H), 4.55 (d, $J = 9.4$ Hz, 1H), 4.46–4.41 (m, 2H), 4.36 (s, 2H), 4.25–4.20 (m, 2H), 4.05–4.00 (m, 1H), 3.94 (s, 3H), 3.66 (q, $J = 10.7, 8.7$ Hz, 3H), 3.24 (s, 3H), 2.97 (s, 2H), 2.94 (d, $J = 6.8$ Hz, 2H), 2.44 (s, 3H), 2.27 (dt, $J = 14.7, 7.6$ Hz, 1H), 2.12 (dd, $J = 14.2, 7.5$ Hz, 1H), 2.01 (dd, $J = 23.6, 9.1$ Hz, 4H), 1.95–1.84 (m, 5H), 1.81–1.73 (m, 4H), 1.62 (dt, $J = 19.3, 5.9$ Hz, 6H), 1.49 (dq, $J = 21.4, 6.8$ Hz, 2H), 1.31–1.23 (m, 6H), 0.94 (s, 9H), 0.76 (t, $J = 7.5$ Hz, 3H). ^{13}C NMR (151 MHz, DMSO- d_6) δ 172.10, 171.98, 169.73, 165.60, 163.18, 151.47, 146.65, 138.30, 132.37, 131.19, 129.65, 128.65, 127.44, 120.34, 116.17, 115.92, 68.89, 59.76, 58.73, 58.31, 56.39, 56.31, 56.10, 41.67, 38.01, 35.26, 34.84, 28.79, 28.49, 28.31, 26.50, 26.41, 26.13, 25.32, 23.57, 23.29, 23.01, 15.96, 8.88. HRMS (ESI) m/z : [M + H] $^+$ calculated for $\text{C}_{58}\text{H}_{80}\text{N}_{11}\text{O}_7\text{S}$ 1062.5963, found 1062.5939. HPLC (purity): 98.86 % ($\lambda = 254$ nm, $t_{\text{R}} = 12.276$ min).

4.7.15. (2S,4R)-1-((S)-2-(10-(4-(4-((R)-8-cyclopentyl-7-ethyl-5-methyl-6-oxo-5,6,7,8-tetrahydropteridin-2-yl)amino)-3-methoxybenzamido) piperidin-1-yl)decanamido)-3,3-dimethylbutanoyl)-4-hydroxy-N-(4-(4-methylthiazol-5-yl)benzyl)pyrrolidine-2-carboxamide (14d)

Compound 14d (10 mg, yield: 30 %) was obtained as a yellow powder using the procedure employed for the synthesis of compound 14a. ^1H NMR (600 MHz, DMSO- d_6) δ 8.98 (s, 1H), 8.56 (t, $J = 6.1$ Hz, 1H), 8.42 (d, $J = 8.3$ Hz, 1H), 8.18 (s, 1H), 8.16 (s, 1H), 7.85 (d, $J = 6.8$ Hz, 2H), 7.61 (s, 1H), 7.49 (d, $J = 10.1$ Hz, 2H), 7.42 (d, $J = 8.3$ Hz, 2H), 7.38 (d, $J = 8.3$ Hz, 2H), 5.16 (s, 1H), 4.55 (d, $J = 9.4$ Hz, 1H), 4.47–4.40 (m, 2H), 4.35 (t, $J = 7.7$ Hz, 2H), 4.22 (dd, $J = 22.7, 4.5$ Hz, 2H), 3.94 (s, 3H), 3.91–3.85 (m, 1H), 3.70–3.62 (m, 3H), 3.24 (s, 3H), 3.15 (d, $J = 10.6$ Hz, 2H), 2.60 (s, 2H), 2.44 (s, 3H), 2.26 (dt, $J = 14.7, 7.7$ Hz,

1H), 2.15 – 2.08 (m, 1H), 2.02 (d, $J = 7.7$ Hz, 2H), 1.96 – 1.83 (m, 5H), 1.83 – 1.75 (m, 4H), 1.74 – 1.55 (m, 6H), 1.55 – 1.42 (m, 4H), 1.30 – 1.20 (m, 10H), 0.94 (s, 9H), 0.76 (t, $J = 7.5$ Hz, 3H). ^{13}C NMR (151 MHz, DMSO- d_6) δ 172.11, 162.94, 151.51, 146.65, 139.52, 138.32, 120.18, 116.15, 115.92, 109.26, 68.88, 59.76, 58.71, 58.30, 56.36, 56.28, 56.06, 51.61, 41.65, 37.98, 35.24, 34.88, 28.84, 28.77, 28.73, 28.67, 28.48, 27.81, 26.55, 26.49, 26.39, 25.44, 25.13, 23.28, 23.00, 15.95, 8.88. HRMS (ESI) m/z : $[\text{M} + \text{H}]^+$ calculated for $\text{C}_{58}\text{H}_{84}\text{N}_{11}\text{O}_7\text{S}$ 1090.6276, found 1090.6246. HPLC (purity): 99.39 % ($\lambda = 254$ nm, $t_{\text{R}} = 12.911$ min).

4.7.16. 7-bromoheptanoyl chloride

A solution of 7-bromoheptanoic acid (250 mg, 1.2 mmol) in thionyl chloride (10 mL) was stirred at 70 °C for 5 h. The reaction mixture was evaporated in vacuum to give the desired product as a brown oil (200 mg).

4.7.17. 8-bromooctanoyl chloride

8-bromooctanoyl chloride (250 mg) was obtained as a yellow powder using the procedure employed for the synthesis of compound 7-bromoheptanoyl chloride.

4.7.18. 10-bromodecanoyl chloride

10-bromodecanoyl chloride (300 mg) was obtained as a yellow powder using the procedure employed for the synthesis of compound 7-bromoheptanoic acid.

4.7.19. 7-bromo-*N*-(2-(2,6-dioxopiperidin-3-yl)-1,3-dioxoisindolin-4-yl)heptanamide (16a)

To a solution of 7-bromoheptanoyl chloride (200 mg, 0.89 mmol) in anhydrous THF (10 mL) was added compound 15 (109 mg, 0.40 mmol), the mixture was heated with stirring at 72 °C for 3h. The reaction was evaporated under reduced pressure to remove THF. The crude product was mixture with methyl *tert*-butyl ether (10 mL) and filtrated, precipitate was washed with methyl *tert*-butyl ether and dried under vacuum to give intermediate compound 16a as gray solid (200 mg, yield: 48 %). ^1H NMR (400 MHz, DMSO- d_6) δ 11.17 (s, 1H), 9.72 (s, 1H), 8.45 (d, $J = 8.4$ Hz, 1H), 7.83 (t, $J = 7.8$ Hz, 1H), 7.62 (d, $J = 7.2$ Hz, 1H), 5.15 (dd, $J = 12.7$, 5.4 Hz, 1H), 3.53 (t, $J = 6.6$ Hz, 2H), 2.90 (ddd, $J = 17.8$, 13.6, 5.3 Hz, 1H), 2.65 – 2.52 (m, 2H), 2.46 (d, $J = 7.4$ Hz, 2H), 2.07 (dd, $J = 11.6$, 5.7 Hz, 1H), 1.80 (p, $J = 6.8$ Hz, 2H), 1.62 (h, $J = 6.4$, 5.4 Hz, 2H), 1.39 (dp, $J = 22.1$, 7.3 Hz, 4H). ^{13}C NMR (151 MHz, DMSO- d_6) δ 172.88, 172.08, 169.88, 167.72, 166.76, 136.56, 136.19, 131.52, 126.48, 117.16, 69.78, 48.97, 35.22, 32.13, 30.99, 27.63, 27.30, 26.14, 24.66. ESI $m/z = 464.50$ $[\text{M} + \text{H}]^+$.

4.7.20. 8-bromo-*N*-(2-(2,6-dioxopiperidin-3-yl)-1,3-dioxoisindolin-4-yl)octanamide (16b)

Compound 16b (100 mg, yield: 25 %) was obtained as a yellow powder using the procedure employed for the synthesis of compound 16a. ^1H NMR (400 MHz, DMSO- d_6) δ 11.17 (s, 1H), 9.71 (s, 1H), 8.46 (d, $J = 8.4$ Hz, 1H), 7.83 (t, $J = 7.8$ Hz, 1H), 7.61 (d, $J = 7.2$ Hz, 1H), 5.15 (dd, $J = 12.8$, 5.4 Hz, 1H), 3.52 (t, $J = 6.7$ Hz, 2H), 2.89 (ddd, $J = 17.0$, 13.7, 5.2 Hz, 1H), 2.64 – 2.51 (m, 2H), 2.46 (t, $J = 7.4$ Hz, 2H), 2.10 – 1.97 (m, 1H), 1.65 – 1.57 (m, 2H), 1.51 (d, $J = 6.4$ Hz, 2H), 1.39 – 1.27 (m, 6H). ^{13}C NMR (151 MHz, DMSO- d_6) δ 172.86, 172.12, 169.86, 167.76, 166.75, 136.59, 136.19, 131.50, 126.37, 118.39, 117.05, 69.78, 48.97, 36.51, 32.23, 31.00, 28.37, 27.85, 26.14, 22.05. ESI $m/z = 478.25$ $[\text{M} + \text{H}]^+$.

4.7.21. 10-bromo-*N*-(2-(2,6-dioxopiperidin-3-yl)-1,3-dioxoisindolin-4-yl)decanamide (16c)

Compound 16c (100 mg, yield: 27 %) was obtained as a yellow powder using the procedure employed for the synthesis of compound 16a. ^1H NMR (400 MHz, DMSO- d_6) δ 11.17 (s, 1H), 9.70 (s, 1H), 8.46 (d, $J = 8.4$ Hz, 1H), 7.83 (dd, $J = 8.4$, 7.3 Hz, 1H), 7.61 (d, $J = 7.2$ Hz, 1H),

5.15 (dd, $J = 12.8$, 5.4 Hz, 1H), 3.51 (t, $J = 6.7$ Hz, 2H), 2.96 – 2.82 (m, 1H), 2.68 – 2.51 (m, 2H), 2.45 (t, $J = 7.4$ Hz, 2H), 2.10 – 2.01 (m, 1H), 1.77 (p, $J = 6.8$ Hz, 2H), 1.66 – 1.56 (m, 2H), 1.41 – 1.21 (m, 10H). ^{13}C NMR (151 MHz, DMSO- d_6) δ 173.27, 172.55, 170.27, 168.15, 137.00, 136.59, 131.91, 126.77, 117.46, 49.37, 36.98, 35.70, 32.68, 31.39, 29.17, 29.06, 28.89, 28.49, 27.94, 25.23, 22.45. ESI $m/z = 506.42$ $[\text{M} + \text{H}]^+$.

4.7.22. 4-(((*R*)-8-cyclopentyl-7-ethyl-5-methyl-6-oxo-5,6,7,8-tetrahydropteridin-2-yl)amino)-*N*-(1-(7-((2-(2,6-dioxopiperidin-3-yl)-1,3-dioxoisindolin-4-yl)amino)-7-oxoheptyl)piperidin-4-yl)-3-methoxybenzamide (17a)

To a solution of compound 16a (20 mg, 0.030 mmol) and Compound 11 (24 mg, 0.045 mmol) in DMF were added K_2CO_3 (8 mg, 0.06 mmol, 2.0 equiv), the reaction mixture was then stirred at 60 °C for 3 h. The resulting mixture was purified by preparative HPLC (5 %–100 % acetonitrile plus 0.1 % formic acid / 0.1 % water plus 0.1 % formic acid). The product containing fractions were concentrated to remove the organic solvent under reduced pressure and then dried by lyophilization to afford compound 17a as white solid (20 mg, yield: 52 %). ^1H NMR (400 MHz, DMSO- d_6) δ 11.18 (s, 1H), 9.72 (s, 1H), 8.46 (d, $J = 8.3$ Hz, 1H), 8.41 (d, $J = 8.9$ Hz, 1H), 8.24 (s, 1H), 8.09 (d, $J = 7.8$ Hz, 1H), 7.88 – 7.79 (m, 2H), 7.65 – 7.57 (m, 2H), 7.52 – 7.46 (m, 2H), 5.15 (dd, $J = 12.7$, 5.5 Hz, 1H), 4.40 – 4.29 (m, 1H), 4.24 (d, $J = 7.6$ Hz, 1H), 3.93 (s, 3H), 3.75 (d, $J = 12.7$ Hz, 2H), 3.24 (s, 3H), 2.88 (d, $J = 11.1$ Hz, 2H), 2.60 (d, $J = 16.5$ Hz, 1H), 2.45 (d, $J = 7.4$ Hz, 2H), 2.32 – 2.23 (m, 2H), 2.15 – 1.93 (m, 4H), 1.89 (s, 2H), 1.77 (d, $J = 10.5$ Hz, 6H), 1.68 – 1.44 (m, 8H), 1.44 (d, $J = 6.3$ Hz, 2H), 1.32 (d, $J = 10.2$ Hz, 4H), 0.76 (t, $J = 7.4$ Hz, 3H). ^{13}C NMR (151 MHz, DMSO- d_6) δ 172.80, 171.99, 169.82, 166.68, 162.96, 151.53, 146.69, 136.53, 136.17, 59.76, 58.30, 56.08, 48.92, 36.38, 30.95, 28.77, 28.49, 28.09, 26.49, 24.56, 23.30, 23.02, 22.00, 8.89. HRMS (ESI) m/z : $[\text{M} + \text{H}]^+$ calculated for $\text{C}_{47}\text{H}_{59}\text{N}_{10}\text{O}_8$ 891.4517, found 891.4471. HPLC (purity): 98.52 % ($\lambda = 254$ nm, $t_{\text{R}} = 11.767$ min).

4.7.23. 4-(((*R*)-8-cyclopentyl-7-ethyl-5-methyl-6-oxo-5,6,7,8-tetrahydropteridin-2-yl)amino)-*N*-(1-(8-((2-(2,6-dioxopiperidin-3-yl)-1,3-dioxoisindolin-4-yl)amino)-8-oxooctyl)piperidin-4-yl)-3-methoxybenzamide (17b)

Compound 17b (15 mg, yield: 41 %) was obtained as a yellow powder using the procedure employed for the synthesis of compound 17a. ^1H NMR (400 MHz, DMSO- d_6) δ 11.19 (s, 1H), 9.71 (s, 1H), 8.46 (d, $J = 8.4$ Hz, 1H), 8.41 (d, $J = 8.8$ Hz, 1H), 8.31 (s, 1H), 8.08 (d, $J = 7.9$ Hz, 1H), 7.86 – 7.80 (m, 2H), 7.64 – 7.58 (m, 2H), 7.52 – 7.44 (m, 2H), 5.20 – 5.13 (m, 1H), 4.37 – 4.32 (m, 1H), 4.25 – 4.21 (m, 1H), 3.93 (s, 3H), 3.80 – 3.67 (m, 2H), 3.24 (s, 3H), 2.88 (s, 2H), 2.62 (d, $J = 3.4$ Hz, 1H), 2.45 (d, $J = 7.3$ Hz, 2H), 2.27 (s, 2H), 2.03 (d, $J = 14.2$ Hz, 2H), 1.90 (t, $J = 5.0$ Hz, 4H), 1.76 (d, $J = 9.5$ Hz, 6H), 1.66 – 1.53 (m, 8H), 1.42 (s, 2H), 1.31 (d, $J = 11.0$ Hz, 6H), 0.76 (t, $J = 7.4$ Hz, 3H). ^{13}C NMR (151 MHz, DMSO- d_6) δ 172.80, 172.03, 169.82, 167.74, 166.68, 162.96, 154.30, 151.53, 146.68, 138.31, 136.55, 136.16, 126.39, 126.29, 120.24, 118.37, 116.18, 115.93, 109.32, 59.76, 58.30, 56.09, 48.93, 36.48, 30.95, 28.78, 28.49, 28.29, 27.83, 26.49, 26.06, 24.65, 23.30, 22.00. HRMS (ESI) m/z : $[\text{M} + \text{H}]^+$ calculated for $\text{C}_{48}\text{H}_{61}\text{N}_{10}\text{O}_8$ 905.4674, found 905.4656. HPLC (purity): 99.81 % ($\lambda = 254$ nm, $t_{\text{R}} = 12.214$ min).

4.7.24. 4-(((*R*)-8-cyclopentyl-7-ethyl-5-methyl-6-oxo-5,6,7,8-tetrahydropteridin-2-yl)amino)-*N*-(1-(10-((2-(2,6-dioxopiperidin-3-yl)-1,3-dioxoisindolin-4-yl)amino)-10-oxodecyl)piperidin-4-yl)-3-methoxybenzamide (17c)

Compound 17c (10 mg, yield: 27 %) was obtained as a yellow powder using the procedure employed for the synthesis of compound 17a. ^1H NMR (400 MHz, DMSO- d_6) δ 11.21 (s, 1H), 9.71 (s, 1H), 8.45 (s, 1H), 8.41 (d, $J = 8.8$ Hz, 1H), 8.19 (s, 1H), 8.11 (d, $J = 7.7$ Hz, 1H), 7.87 – 7.79 (m, 2H), 7.61 (d, $J = 7.3$ Hz, 2H), 7.52 – 7.43 (m, 2H), 5.15 (dd, J

= 12.8, 5.4 Hz, 1H), 4.39–4.31 (m, 1H), 4.24 (dd, $J = 7.5, 3.5$ Hz, 1H), 3.93 (s, 3H), 3.82–3.73 (m, 2H), 3.24 (s, 3H), 2.92 (d, $J = 8.9$ Hz, 2H), 2.64–2.58 (m, 1H), 2.46 (t, $J = 7.4$ Hz, 2H), 2.31 (t, $J = 7.4$ Hz, 2H), 2.03 (q, $J = 10.9, 8.1$ Hz, 4H), 1.88 (d, $J = 7.9$ Hz, 2H), 1.77 (tq, $J = 7.5, 4.0$ Hz, 6H), 1.60 (tt, $J = 9.9, 5.2$ Hz, 8H), 1.42 (t, $J = 7.2$ Hz, 2H), 1.28 (d, $J = 14.3$ Hz, 10H), 0.76 (t, $J = 7.4$ Hz, 3H). ^{13}C NMR (151 MHz, DMSO- d_6) δ 172.78, 172.06, 169.80, 167.70, 166.68, 165.13, 162.94, 154.33, 151.51, 146.64, 138.34, 136.56, 136.12, 132.15, 131.47, 126.70, 126.28, 120.11, 118.31, 116.12, 115.94, 109.21, 59.77, 58.31, 56.05, 48.91, 46.73, 30.95, 28.88, 28.76, 28.70, 28.49, 27.81, 26.87, 26.48, 26.28, 24.79, 23.26, 22.99, 21.99, 8.88. HRMS (ESI) m/z : $[\text{M} + \text{H}]^+$ calculated for $\text{C}_{47}\text{H}_{65}\text{N}_{10}\text{O}_8$ 933.4987, found 933.4966. HPLC (purity): 99.55 % ($\lambda = 254$ nm, $t_{\text{R}} = 13.138$ min).

4.8. Statistical analysis

Statistical analysis was performed using GraphPad Prism 9.4.1, data were presented as mean \pm standard deviation, P-values were calculated using the two-way ANOVA with Tukey's multiple comparison test, $P < 0.05$ was considered to be statistically significant.

Author contributions

S. Song synthesized the compounds, and performed the majority of biological evaluation. W. Yang participated in the in vitro evaluation of cytotoxicity. W. Tai supervised the study and provided funding resources.

CRedit authorship contribution statement

Shiwei Song: Writing – original draft, Methodology, Investigation, Data curation, Conceptualization. **Wanrong Yang:** Methodology, Investigation. **Wanyi Tai:** Writing – review & editing, Supervision, Conceptualization.

Declaration of competing interest

The authors declare that they have no known competing financial interests or personal relationships that could have appeared to influence the work reported in this paper.

Acknowledgement

Authors acknowledge Sibao Jiang of Changsha Medical University for their work on chemical structure analysis and writing support. This work was financially supported by the National Key R&D Program of China (Grant No. 2021YFA0909900) and the National Natural Science Foundation of China (Grant No. 82273860).

Appendix A. Supplementary data

Supplementary data to this article can be found online at <https://doi.org/10.1016/j.bmc.2025.118087>.

Data availability

No data was used for the research described in the article.

References

- Zheng L, Wang W, Sun Q. Targeted drug approvals in 2023: breakthroughs by the FDA and NMPA. *Signal Transduction and Targeted Therapy*. 2024;9:46.
- Li K, Crews CM. PROTACs: past, present and future. *Chemical Society Reviews*. 2022; 51:5214–5236.
- Sakamoto KM, Kim KB, Kumagai A, Mercurio F, Crews CM, Deshaies RJ. Protacs: chimeric molecules that target proteins to the Skp1-Cullin-F box complex for

- ubiquitination and degradation. *Proceedings of the National Academy of Sciences of the United States of America*. 2001;98:8554–8559.
- Crew AP, Raina K, Dong H, et al. Identification and Characterization of Von Hippel-Lindau-Recruiting Proteolysis Targeting Chimeras (PROTACs) of TANK-Binding Kinase 1. *Journal of Medicinal Chemistry*. 2018;61:583–598.
- Békés M, Langley DR, Crews CM. PROTAC targeted protein degraders: the past is prologue. *Nature Reviews. Drug Discovery*. 2022;21:181–200.
- Khan S, He Y, Zhang X, et al. PROTeolysis TARgeting Chimeras (PROTACs) as emerging anticancer therapeutics. *Oncogene*. 2020;39:4909–4924.
- Zhao L, Zhao J, Zhong K, Tong A, Jia D. Targeted protein degradation: mechanisms, strategies and application. *Signal Transduction and Targeted Therapy*. 2022;7:113.
- Guharoy M, Bhowmick P, Sallam M, Tompa P. Tripartite degrons confer diversity and specificity on regulated protein degradation in the ubiquitin-proteasome system. *Nature Communications*. 2016;7:10239.
- Wang S, He F, Tian C, Sun A. From PROTAC to TPD: Advances and Opportunities in Targeted Protein Degradation. *Pharmaceuticals*. 2024;17:100.
- Yang CY, Qin C, Bai L, Wang S. Small-molecule PROTAC degraders of the Bromodomain and Extra Terminal (BET) proteins - A review. *Drug Discovery Today: Technologies*. 2019;31:43–51.
- Belkina AC, Denis GV. BET domain co-regulators in obesity, inflammation and cancer. *Nature Reviews. Cancer*. 2012;12:465–477.
- Nicodeme E, Jeffrey KL, Schaefer U, et al. Suppression of inflammation by a synthetic histone mimic. *Nature*. 2010;468:1119–1123.
- Chirnomas D, Hornberger KR, Crews CM. Protein degraders enter the clinic - a new approach to cancer therapy. *Nature Reviews. Clinical Oncology*. 2023;20:265–278.
- Zhang D, Baek SH, Ho A, Lee H, Jeong YS, Kim K. Targeted degradation of proteins by small molecules: a novel tool for functional proteomics. *Combinatorial Chemistry & High Throughput Screening*. 2004;7:689–697.
- Lam LT, Lin X, Faivre EJ, et al. Vulnerability of Small-Cell Lung Cancer to Apoptosis Induced by the Combination of BET Bromodomain Proteins and BCL2 Inhibitors. *Molecular Cancer Therapeutics*. 2017;16:1511–1520.
- Iliaki S, Beyaert R, Afonina IS. Polo-like kinase 1 (PLK1) signaling in cancer and beyond. *Biochemical Pharmacology*. 2021;193, 114747.
- Zhang J, Zhang L, Wang J, Ouyang L, Wang Y. Polo-like Kinase 1 Inhibitors in Human Cancer Therapy: Development and Therapeutic Potential. *Journal of Medicinal Chemistry*. 2022;65:10133–10160.
- Pezuk JA, Brassesco MS, Oliveira JC, et al. Antiproliferative in vitro effects of BI 2536-mediated PLK1 inhibition on cervical adenocarcinoma cells. *Clinical and Experimental Medicine*. 2013;13:75–80.
- Liu S, Yosief HO, Dai L, et al. Structure-Guided Design and Development of Potent and Selective Dual Bromodomain 4 (BRD4)/Polo-like Kinase 1 (PLK1) Inhibitors. *Journal of Medicinal Chemistry*. 2018;61:7785–7795.
- Mu X, Bai L, Xu Y, Wang J, Lu H. Protein targeting chimeric molecules specific for dual bromodomain 4 (BRD4) and Polo-like kinase 1 (PLK1) proteins in acute myeloid leukemia cells. *Biochemical and Biophysical Research Communications*. 2020; 521:833–839.
- Hu R, Wang WL, Yang YY, et al. Identification of a selective BRD4 PROTAC with potent antiproliferative effects in AR-positive prostate cancer based on a dual BET/PLK1 inhibitor. *European Journal of Medicinal Chemistry*. 2022;227, 113922.
- Gunasekaran, P.; Hwang, Y. S.; Lee, G.-H.; Park, J.; Kim, J. G.; La, Y. K.; Park, N. Y.; Kothandaraman, R.; Yim, M. S.; Choi, J.; Kim, H. N.; Park, I. Y.; Lee, S. J.; Kim, M.-H.; Cha-Molstad, H.; Shin, S. Y.; Ryu, E. K.; Bang, J. K. Dihydropteridines, prodode de production et utilisation de ces dernieres comme medicaments. 2003, Patent CA2517020C.
- Gandhi AK, Kang J, Havens CG, et al. Immunomodulatory agents lenalidomide and pomalidomide co-stimulate T cells by inducing degradation of T cell repressors Ikaros and Aiolos via modulation of the E3 ubiquitin ligase complex CRL4(CRBN). *British Journal of Haematology*. 2014;164:811–821.
- Ember SW, Zhu JY, Olesen SH, et al. Acetyl-lysine binding site of bromodomain-containing protein 4 (BRD4) interacts with diverse kinase inhibitors. *ACS Chemical Biology*. 2014;9:1160–1171.
- Lénárt P, Petronczki M, Stegmaier M, et al. The small-molecule inhibitor BI 2536 reveals novel insights into mitotic roles of polo-like kinase 1. *Current Biology*. 2007; 17:304–315.
- Kothe M, Kohls D, Low S, et al. Selectivity-determining residues in Plk1. *Chemical Biology & Drug Design*. 2007;70:540–546.
- Ciceri P, Müller S, O'Mahony A, et al. Dual kinase-bromodomain inhibitors for rationally designed polypharmacology. *Nature Chemical Biology*. 2014;10:305–312.
- Chen L, Yap JL, Yoshioka M, et al. BRD4 Structure-Activity Relationships of Dual PLK1 Kinase/BRD4 Bromodomain Inhibitor BI-2536. *ACS Medicinal Chemistry Letters*. 2015;6:764–769.
- Budin G, Yang KS, Reiner T, Weissleder R. Bioorthogonal probes for polo-like kinase 1 imaging and quantification. *Angewandte Chemie (International Ed. in English)*. 2011; 50:9378–9381.
- Devaiah BN, Geggion A, Singer DS. Bromodomain 4: a cellular Swiss army knife. *Journal of Leukocyte Biology*. 2016;100:679–686.
- Li J, Wang R, Kong Y, et al. Targeting Plk1 to Enhance Efficacy of Olaparib in Castration-Resistant Prostate Cancer. *Molecular Cancer Therapeutics*. 2017;16: 469–479.
- Chakraborty G, Armenia J, Mazzu YZ, et al. Significance of BRCA2 and RB1 Co-loss in Aggressive Prostate Cancer Progression. *Clinical Cancer Research*. 2020;26: 2047–2064.
- Gadd MS, Testa A, Lucas X, et al. Structural basis of PROTAC cooperative recognition for selective protein degradation. *Nature Chemical Biology*. 2017;13: 514–521.

34. Troup RI, Fallan C, Baud MGJ. Current strategies for the design of PROTAC linkers: a critical review. *Explor. Target. Antitumor. Ther.* 2020;1:273–312.
35. Taniguchi Y. The Bromodomain and Extra-Terminal Domain (BET) Family: Functional Anatomy of BET Paralogous Proteins. *International Journal of Molecular Sciences.* 2016;17.
36. Shi Y, Liao Y, Liu Q, et al. BRD4-targeting PROTAC as a unique tool to study biomolecular condensates. *Cell Discov.* 2023;9:47.
37. Wang N, Wu R, Tang D, Kang R. The BET family in immunity and disease. *Signal Transduction and Targeted Therapy.* 2021;6:23.
38. Muddassir M, Soni K, Sangani CB, et al. Bromodomain and BET family proteins as epigenetic targets in cancer therapy: their degradation, present drugs, and possible PROTACs. *RSC Advances.* 2020;11:612–636.
39. Gunasekaran P, Hwang YS, Lee G-H, et al. Degradation of Polo-like Kinase 1 by the Novel Poly-Arginine N-Degron Pathway PROTAC Regulates Tumor Growth in Nonsmall Cell Lung Cancer. *Journal of Medicinal Chemistry.* 2024;67:3307–3320.
40. Ma L, Wang J, Zhang Y, et al. BRD4 PROTAC degrader MZ1 exerts anticancer effects in acute myeloid leukemia by targeting c-Myc and ANP32B genes. *Cancer Biology & Therapy.* 2022;23:1–15.